

Dramatic Spectral Evolution of WZ Sagittae during the 2001 Superoutburst

Daisaku NOGAMI

Hida Observatory, Kyoto University, Kamitakara, Gifu 506-1314

nogami@kwasan.kyoto-u.ac.jp

Takashi IJIMA

Astronomical Observatory of Padova, Asiago Section, Osservatorio Astrofisico, I-36012 Asiago (Vi), Italy

ijima@astras.pd.astro.it

(Received 2003 0; accepted 2003 0)

Abstract

We carried out optical spectroscopic observations of the most enigmatic dwarf nova WZ Sge in 11 nights during the 2001 superoutburst. Our observations covered the period from the initial phase several hours before the maximum to the ninth maximum of the rebrightening phase. The first spectrum shows absorption lines of H I (except for H α), He I, and Na I, as well as emission lines of He II, C III/N III, and H α in doubly-peaked shapes. The same spectrum shows the emission lines of C IV and N IV which are the first detection in dwarf novae. The spectral features dramatically changed in various time scales. For example, the peak separations of the emission lines of H I and He II changed from ~ 700 km s $^{-1}$ to ~ 1300 km s $^{-1}$, and one of the peaks dominated over an orbital period in the genuine-superhump era, but the dominant peak interchanged with the orbital phase in the early-superhump era. The lines of H I and He I were in emission at minima of the rebrightening phase (with no high-excitation lines, nor Na I), while they became in absorption at maxima. We report on the observational results in detail and their implications concerning the outburst mechanism, two types of superhumps, and variation of the disk structure.

Key words: accretion, accretion disks — stars: novae, cataclysmic variables — stars: dwarf novae — stars: individual (WZ Sagittae)

1. Introduction

WZ Sge is the prototypical star of WZ Sge-type dwarf novae (Bailey 1979; for a recent review, Kato et al. 2001c). This type of stars is understood as a small group in SU UMa-type dwarf novae, but has unusual characteristics of quite large outburst amplitudes up to ~ 8 mag, extraordinary long recurrence cycles of the outbursts (≥ 10 years), no (or only a few) normal outbursts (see Kato et al. 2001c; Nogami et al. 1997b¹). All the outbursts so far observed in WZ Sge have been so-called superoutbursts in normal SU UMa-type dwarf novae. Thus the nomenclature of outburst will be used instead of superoutburst in the case of WZ Sge stars throughout this paper.

In conjunction with these interesting properties, since WZ Sge is relatively bright, $m_V \sim 15.3$ in quiescence, many researchers have most intensively investigated WZ Sge in a variety of methods, and this star has had a significant effect on many aspects of the study of cataclysmic variable stars. While it is impossible to review all the works related to WZ Sge, we introduce some of most importance.

WZ Sge was first discovered in 1913 as a nova, and the second outburst in 1946 suggested this star to be a recurrent nova (Mayall 1946). This second outburst was observed photometrically (e.g. Himpel 1946;

Stevenson 1950; Eskioglu 1963), and spectroscopically (McLaughlin 1953). McLaughlin (1953) suspected the dwarf nova nature based on the spectra. Kraft (1961) revealed that WZ Sge is a spectroscopic binary with a period of ~ 80 min, and subsequent photometry by Krzeminski (1962) proved this star to be an eclipsing binary star with a period of 81.38 min.

To explain the orbital light curve and the line-profile variation, Krzeminski, Kraft (1964) for the first time built a model of the cataclysmic variable star (CVs) containing a white dwarf primary, a late-type secondary star, and a disk, and deduced binary parameters. Based on this model, short-period CVs including WZ Sge were suggested to evolve by the gravitational wave radiation (Kraft et al. 1962; Paczynski 1967; Faulkner 1971; Vila 1971a; Vila 1971b). Using the observations of eclipses, Warner, Nather (1972) further developed this model by including a notion of the hot spot.

High-speed photometry in quiescence by Robinson et al. (1978) was used to refine the binary parameters and revealed oscillations with the periods of 27.87 sec and 28.98 sec. These oscillations were later interpreted to be due to the magnetized white dwarf (Patterson 1980; see also Nather 1978; Lasota et al. 1999).

The third outburst occurred in 1978, which was observed by optical photometry (e.g. Patterson et al. 1978; Bohusz, Udalski 1979; Heiser, Henry 1979; Brosch 1979; Targan 1979; Patterson et al. 1981), optical spectroscopy

¹ The maximum magnitude of WZ Sge in table 1 in Nogami et al. 1997b should be replaced by $m_o = 8.1$

(Patterson et al. 1978; Crampton et al. 1979; Gilliland, Kemper 1980; Walker, Bell 1980; Ortolani et al. 1980), and ultraviolet spectroscopy by the *IUE* satellite (Fabian et al. 1980; Ortolani et al. 1980; Friedjung 1981). Patterson (1979) suspected the SU UMa nature of WZ Sge, based on the photometric data of this outburst. Using the same data, Patterson et al. (1981) suggested that the photometric behavior agreed with that expected by the enhanced mass transfer model, interpreting that periodic modulations, which are called early superhumps in this paper, were enhanced orbital humps. Bailey (1979) pointed out similarity of the outburst light curve of UZ Boo and WX Cet with that of WZ Sge, and proposed that these stars may form a distinct subgroup of the dwarf novae.

Papaloizou, Pringle (1979) put forward a new model of an apsidal precession disk with eccentric orbits to explain the superhumps observed in WZ Sge and other SU UMa stars.

The orbital period (P_{orb}) of WZ Sge had been the shortest one of the normal hydrogen-rich dwarf novae, although some dwarf novae with slightly shorter P_{orb} has been found very recently (Thorstensen et al. 2002). Its orbital period has put a constraint on the theory of the CV evolution (for a review of the standard theory, see e.g. King 1988). This is still one of the topics which are prosperously investigated at present (Barker, Kolb 2003; and references therein).

The small mass of the secondary star in WZ Sge (for recent works, Steeghs et al. 2001a; Skidmore et al. 2002) has stimulated researchers to survey brown dwarfs in CVs (e.g. Ciardi et al. 1998; Littlefair et al. 2000; Patterson 2001; Mennickent, Diaz 2002; Littlefair et al. 2003).

During the dormancy of WZ Sge after the 1978 outburst, some outbursts of the members of WZ Sge stars have been observed, e.g. the 1992 outburst in HV Vir (Barwig et al. 1992; Leibowitz 1993; Kato et al. 2001c), the 1995 outburst (Pych, Olech 1995; Kato et al. 1996; Howell et al. 1996; Szkody et al. 1996; Patterson et al. 1996; Nogami et al. 1997a) and the 2001 outburst (Ishioka et al. 2002) in AL Com, the 1996–1997 outburst in EG Cnc (Matsumoto et al. 1998; Liu et al. 1998), the 1998 outburst in V592 Her (Kato, Starkey 2002; Mennickent et al. 2002), and the 2000–2001 outburst in RZ Leo (Ishioka et al. 2001a).

Among the peculiar properties of WZ Sge stars in outburst these observations revealed, the definitive behavior commonly seen is the early superhump clearly distinguishable from the genuine (common) superhumps [Kato, Starkey (2002) did not find early superhumps in V592 Cas probably because of lack of observations in the early phase of the outburst]. The early superhumps have doubly-humped shapes in contrast to usually singly-humped shape of the genuine superhumps, and have periods a little, but significantly shorter than the orbital period (see Ishioka et al. 2002). For the early superhumps, some models have been proposed, e.g. an enhanced hotspot model (Patterson et al. 1981), an immature superhump model (Kato et al. 1996), jet or axi-

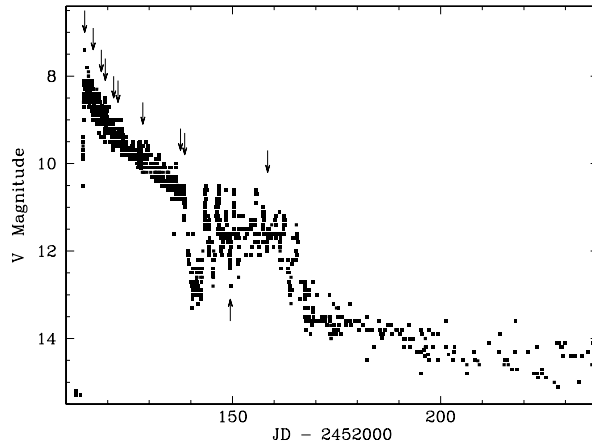


Fig. 1. Long term light curve of the 2001 outburst of WZ Sge. The main outburst lasted about 25 days. After a dip around JD 2452140, WZ Sge caused twelve rebrightenings followed by the long fading tail (see figure 2 in Ishioka et al. 2002, or figure 1 in Patterson et al. 2002). The dots represent the observations reported to VSNET. The arrows point to the times when our observations were carried out.

asymmetrically flared disk models (Nogami et al. 1997a), an irradiated secondary model (Smak 1993).

Theoretical models for the outburst properties mentioned at the top of this section, the outburst mechanisms, and the rebrightening phenomena observed in WZ Sge stars have been also published by many researchers, e.g. Osaki (1995); Warner et al. (1996); Hameury et al. (1997); Meyer-Hofmeister et al. (1998); Mineshige et al. (1998); Hameury et al. (1999); Meyer, Meyer-Hofmeister (1999); Hameury et al. (2000); Montgomery (2001); Lasota (2001); Patterson (2001); Osaki et al. (2001); Hellier (2001); Buat-Ménard et al. (2001); Buat-Ménard, Hameury (2002).

As we have reviewed here, WZ Sge is worthy to be called the *King of dwarf novae*. This dwarf nova gave rise to a new outburst in 2001, 23 years after the previous outburst, and many observation campaigns were immediately organized.

We here report on the results of our spectroscopic observations performed during the fourth outburst in 2001. The next section is devoted to summarize investigations related to this outburst already published. The observations are stated in section 3, and the section 4 describes the results separated into 6 periods. We reconstruct a story of the spectral evolution in section 5, and have discussion regarding the outburst properties, the spectral feature, and the behavior of the accretion disk in section 6. Summary and conclusions are put in the last section 7.

2. 2001 Outburst

The 2001 outburst of WZ Sge (figure 1) was caught by T. Ohshima at 2001 July 23.565 (UT) at $m_{\text{vis}} = 9.7$, which was first reported to Japanese domestic mailing

list by M. Watanabe (vsnet-j 1415)². R. Ishioka (vsnet-alert 6093)³ soon confirmed this outburst and distributed it via VSNET (Kato et al. 2003). Following photometry on the same night revealed further brightening to $m_{\text{vis}} \sim 8.0$ and the presence of early superhumps (Ishioka et al. 2001b; Mattei et al. 2001). Landolt (2001) obtained multi-color photometry: $V \sim 8.26$, $U - B \sim -0.97$, $B - V \sim -0.11$, $V - R \sim -0.02$, $R - I \sim -0.03$ about July 25.20 (UT), bluer than the colors in quiescence (e.g. $B - V = 0.10(5)$, $V - R = 0.16(5)$ in Misselt 1996). Early superhumps were confirmed by Kato et al. (2001a), who measured the period of the early superhump to be 0.056652(6) d from photometric data obtained between July 24.46 and 27.01 (see also Ishioka et al. 2002).

The spectrum at July 23.74 (UT) had absorption lines of $\text{H}\alpha$ and $\text{H}\beta$ superposed on a blue continuum (Ishioka et al. 2001b). In the next night, however, time-resolved spectra acquired by Baba et al. (2001) between July 24.576 and 24.701 (UT) showed an emission component in the $\text{H}\beta$ absorption line varying with its orbital period (see Baba et al. 2002). Doubly-peaked emission lines of $\text{He II } 4686$ and the Bowen blend of C III/N III around 4640 Å were also observed in the same spectra, which were not seen one day before (see figure 1 in Baba et al. 2002). From phase-resolved spectra taken between July 28.02 and 28.24 (UT), Steeghs et al. (2001b) drawn Doppler maps of $\text{He II } 4686$ and $\text{C III } 4647$ which suggested that the accretion-disk emission was dominated by two spiral arms (see Kuulkers et al. 2002).

The observations by the Chandra X-ray Observatory at July 27.11 (UT) were characterized by doubly-peaked modulations of the mean 0th-order count rate with the orbital period and broad (FWHM = 800–1200 km s⁻¹) emission lines of highly ionized species, such as O V-VIII , Ne V-VIII , Mg V-VII , Fe VII-IX (Wheatley et al. 2001). The spectrum observed in their second Chandra observation around July 29.73 (UT) was accounted for with a multi-temperature thermal plasma model with a strong emission line at 2.4 keV, probably He-like S XV .

The early superhumps were superseded by the genuine superhumps with a period of 0.057143(46) d on August 4.53 (UT), 12 days after the start of the outburst (Kato et al. 2001b). The maximum timing of the superhumps systematically fluctuated around a linear ephemeris [$HJD = 2452126.755 + 0.057153(16) \times E$] with a probable period ~ 4 d, which were interpreted by the beat between the orbital and the superhump periods (Kato et al. 2001b). Kato et al. (2001b) also reported that a doubly-peaked profile of the superhump on August 9 was changed to a singly-peaked profile on August 11.

WZ Sge rapidly declined in the early days from the maximum, and the decline then steadily became more gradual. Cannizzo (2001) proved that this trend is a natural result of decrease of the disk mass. Based on the growth of the early superhump amplitude around the supermaximum

and the period of the early superhumps 0.05% longer than P_{orb} , Ishioka et al. (2002) rejected the mass-transfer burst model for the outburst in WZ Sge originally proposed by Patterson et al. (1981).

An asymmetric spiral structure was seen in the Doppler map of the doubly-peaked emission line $\text{He II } 4686$, but not in that of $\text{H}\alpha$, in July 24–27 (Baba et al. 2002). In the emission line $\text{H}\alpha$, Steeghs et al. (2001a) found a narrow emission component from the irradiated secondary star which first appeared in early August. The $\text{H}\alpha$ Doppler map constructed by Steeghs et al. (2001a) from spectra on August 13 indicated that the disk emission was dominated by a strong extended bright spot. This map is much different from those in the early phase of the current outburst presented by Steeghs et al. (2001b) and Baba et al. (2002), but similar to those in quiescence (e.g. Skidmore et al. 2000).

Quite intensive photometric observations were carried out throughout the entire outburst with the long fading tail lasting over 100 days, which are summarized by Patterson et al. (2002) and Ishioka et al. (2004). They report a variety of photometric behavior in unprecedented detail, such as early superhumps, common superhumps, development and decay of these two types of humps, eclipses with a nature different from that in quiescence, 12 repetitive brightenings following the 3-days dip after the main outburst, superhumps in the long fading tail. The limits on the masses were derived by Patterson et al. (2002) to be $M_1 > 0.8M_{\odot}$ and $M_2 < 0.08M_{\odot}$.

Howell et al. (2003) obtained time-resolved infrared spectra on 2001 July 27, which contained emission lines of H , He I , He II , Fe I , Na I , Ca I , C I . Doppler maps of $\text{Pa}\beta$, $\text{Pa}\gamma$, He I , and He II drawn from their spectra showed spiral structures sharing the same feature with that of $\text{He II } 4686$ in optical (Baba et al. 2002). However, the component with $v_x > 0$ km s⁻¹ was dominant in the maps of $\text{Pa}\beta$, $\text{Pa}\gamma$, and He I .

Far-ultraviolet observations during and after the 2001 outburst were carried out with the *Far Ultraviolet Spectroscopic Explorer* (FUSE) (Long et al. 2003) and the *Hubble Space Telescope* (HST) (Knigge et al. 2002; Sion et al. 2003). The FUSE spectra on the 7th day of the outburst contained a strong O IV absorption line with a blue-shifted core and the absorption lines of moderate ionization-state ions. These lines suggest an outflow and a tenuous layer above the disk (or a vertically extended disk), which is supported by the HST observations by Sion et al. (2003). Long et al. (2003) also estimated the mass of the white dwarf to be $0.8 M_{\odot}$, or larger, which is consistent with the results by Skidmore et al. (2000), Steeghs et al. (2001a) and Patterson et al. (2002). Knigge et al. (2002) observed WZ Sge on 2001 August 8 (plateau phase), 19 (dip), 22 (just after the first peak during the rebrightening). Among three data sets, the August 22 one indicated 15-sec oscillations, similar to those seen in quiescence (Provencal, Nather 1997). Possible 6.5-sec oscillations on the same night were first time seen in the history of the WZ Sge study. Nevertheless, these oscillations were not caught on August 8 and 19. Knigge et al. (2002) did

² (<http://vsnet.kusastro.kyoto-u.ac.jp/vsnet/Mail/j1000/msg00415.html>).

³ (<http://vsnet.kusastro.kyoto-u.ac.jp/vsnet/Mail/alert6000/msg00093.html>).

not find evidence of 29-sec signals which had been detected by Robinson et al. (1978), Patterson (1980), Skidmore et al. (1997), Welsh et al. (1997), Patterson et al. (1998b), Skidmore et al. (1999), and Skidmore et al. (2002).

Based on the detailed observations of the early superhumps presented by Ishioka et al. (2002) and Patterson et al. (2002), two new models have been proposed by Osaki, Meyer (2002) and Kato (2002a). Osaki, Meyer (2002) described that early superhumps can be explained by tidal removal of the angular momentum from the accretion disk by the 2:1 resonance (Lin, Papaloizou 1979)⁴. The model by Kato (2002a) is an application of the tidal distortion effect in the accretion disk (see Smak 2002; Ogilvie 2002).

Osaki, Meyer (2003) critically examined the “observed” evidence of enhanced mass transfer including that proposed by Patterson et al. (2002), and argued that the overall light curve of the 2001 outburst does not require an assumption of enhanced mass transfer in the scheme of the thermal-tidal disk instability model.

Being inspired by the complex superhump light curves observed during the 2001 outburst in WZ Sge, Osaki (2003) proposed a new method “helical tomography”, to analyze superhump light curves of SU UMa stars with high orbital inclination.

3. Observation

We obtained 83 optical spectra in total in 11 nights during the 2001 outburst (figure 1). Table 1 gives a journal of the observations. The spectra of a medium resolution ($\sim 6 \text{ \AA}$) were taken with a Boller & Chivens spectrograph mounted on the 122-cm telescope of the Asiago Astrophysical Observatory of the University of Padova, using a 512×512 -pixel CCD detector. An echelle spectrograph on the 182-cm telescope of Mount Ekar station of the Astronomical Observatory of Padova and a CCD camera of 550×550 pixels were used to obtain the high-dispersion spectroscopy (resolution 0.6 \AA).

The spectra were reduced in the standard ways using the IRAF package⁵ at the Asiago Observatory. The sensitivity of the spectrographs were corrected using spectra of some spectrophotometric standard stars (BD+25 3941 and HD 192281 for the medium dispersion spectroscopy, and 58 Aql for the high dispersion spectroscopy) obtained in the same nights. The signal-to-noise ratio at the continuum varies over 100 to ~ 20 , depending on the sky condition, the exposure time, and, most significantly, the object brightness. The orbital phase ϕ , which is used throughout this paper, is calculated with the following ephemeris:

$$\phi = \frac{\text{BJD} - T_0}{P_{\text{orb}}} - \phi_{\text{cor}} - E_0, \quad (1)$$

⁴ Interestingly, Lin, Papaloizou (1979) originally introduced the idea of a spiral dissipation pattern due to the 2:1 resonance to explain the doubly-peaked shape of the orbital humps of WZ Sge observed in quiescence.

⁵ IRAF is distributed by the National Optical Astronomy Observatories for Research in Astronomy, Inc. under cooperative agreement with the National Science Foundation.

where $T_0 = 2437547.728868$, $P_{\text{orb}} = 0.05668784707$, and $\phi_{\text{cor}} = -0.022$ (see Skidmore et al. 2000). The E_0 is set to be 256964 in order that the orbital phase in this paper starts around $\phi = 0$.

4. Results

In this section, we describe detailed spectral feature, separating our observations into six periods. As in table 1, period I is the very early phase of the outburst from JD 2452114 to 2452118, period II is from 2452119 to 2452122, period III is on JD 2452128, period IV is the end of the main outburst on JD 2452137 and 2452138, period V is in the third minimum in the rebrightening stage on JD 2452149, and period VI is at the 9th rebrightening peak on JD 2452158.

4.1. Period I (JD 2452114–2452118, 1st–5th day)

The spectra obtained on JD 2452114 just around the outburst maximum are shown in figure 2. The continuum flux in figure 2b seems higher than those in Figure 2a and 2c. This discrepancy should represent intrinsic modulations of the continuum, since the amplitude of the early superhump were about 0.5 mag around those observations (Ishioka et al. 2004). The error of the flux calibration is within 10 %.

The continuum is very blue, and deep Balmer (except for $H\alpha$ in emission) and He I absorption lines are superposed on it, while He II and the C III/N III Bowen blend are in emission. Note that the strong high-excitation emission lines C IV 5802/5813 and N IV 5786/5796 are also present, which were first caught in dwarf novae.

Figure 3 exhibits the spectra obtained by averaging all the spectra obtained during the period I after normalization at the continuum level. $H\alpha$ and He II are in doubly-peaked emission. The peak separations in the spectra where the blue- and red-peak wavelengths are easily measured by Gaussian fitting are summarized in table 2. Those of $H\alpha$ and He II 4686 were rather small, $\sim 700 \text{ km s}^{-1}$, in the first night, then gradually increased. The broadening rate was larger in He II 4686 than in $H\alpha$. In contrast, the separation of He II 5411 was large since its emergence. The C IV and N IV emission lines were observed on JD 2452114 and 2452116. These emission lines were, however, not detected, or at least quite weak, on JD 2452128 and later. Note that the Na I D 5890/5896 absorption lines were also clearly present from our first run, while it suffered from significant contamination of He I 5875. These high-excitation lines and Na I features do not exist in optical quiescence spectra (see e.g. Gilliland et al. 1986).

The daily averaged line fluxes and equivalent widths (EWs) of emission lines (C III/N III, He II 4686, C IV/N IV complex, and $H\alpha$) are listed in table 3. It is difficult to separate C III/N III and He II, as seen in figure 3. In this measurement, we simply accumulated the flux in the bluer region of the trough between the red peak of C III/N III and the blue peak of He II as the C III/N III line flux and in the redder region for He II. As for the C IV/N IV

Table 1. Log of the observations.

Date	Start UT	Exposure Time(s)	File ID	Mid BJD (2400000+)	Orbital Phase	Instr.	Spectral Range (Å)	Period	Comments	
Jul.	23	23:18	300	10550	52114.47802	0.255	B&C	3942–5130	I	
		23:41	300	10553	52114.49368	0.531	"	4844–6041	"	
	24	00:08	60	10557	52114.51157	0.847	"	5698–6901	"	
		00:10	300	10558	52114.51437	0.896	"	"	"	
	25	22:49	300	10562	52116.45794	35.182	"	3984–5173	"	cloudy
	26	00:03	300	10564	52116.50894	36.081	"	"	"	
		00:40	300	10568	52116.53492	36.540	"	4767–5963	"	
		02:11	180	10577	52116.59774	37.648	"	5818–7021	"	
		02:15	300	10578	52116.60102	37.706	"	"	"	
		02:25	600	10580	52116.60967	37.858	"	3983–5173	"	
	27	21:30	600	10585	52118.40481	69.525	"	3985–5174	"	
		21:57	600	10588	52118.42319	69.850	"	"	"	
		23:39	600	10595	52118.49438	71.106	"	"	"	cloudy
		23:54	300	10597	52118.50300	71.258	"	5771–6974	"	
	28	01:43	300	10603	52118.57875	72.594	"	"	"	
		22:48	600	10613	52119.45913	88.124	"	3937–5125	II	cloudy
	30	21:38	360	10616	52121.40921	122.525	"	3924–5111	"	
		21:48	600	10618	52121.41743	122.670	"	"	"	
		22:20	360	10620	52121.43779	123.029	"	"	"	
		22:28	360	10622	52121.44388	123.136	"	"	"	
		22:37	360	10624	52121.44961	123.237	"	"	"	
		22:43	360	10625	52121.45427	123.319	"	"	"	
		22:53	360	10626	52121.46127	123.443	"	"	"	
		23:02	360	10628	52121.46729	123.549	"	"	"	
		23:09	360	10629	52121.47199	123.632	"	"	"	
		23:16	360	10630	52121.47708	123.722	"	"	"	
		23:23	360	10631	52121.48152	123.800	"	"	"	
	31	21:43	600	10637	52122.41396	140.249	"	4038–5227	"	
		21:56	600	10639	52122.42288	140.406	"	"	"	cloudy
		22:09	600	10640	52122.43203	140.568	"	"	"	
		22:21	600	10642	52122.44016	140.711	"	"	"	
		22:33	600	10644	52122.44844	140.857	"	"	"	
		22:43	600	10645	52122.45578	140.987	"	"	"	
		22:54	600	10646	52122.46309	141.116	"	"	"	
		23:06	600	10648	52122.47153	141.264	"	"	"	
		23:17	600	10649	52122.47887	141.394	"	"	"	
		23:27	600	10650	52122.48619	141.523	"	"	"	
Aug.	1	00:00	300	10654	52122.50691	141.889	"	5775–6979	"	
		00:07	360	10656	52122.51234	141.984	"	"	"	
		00:13	360	10657	52122.51670	142.061	"	"	"	
		00:20	360	10658	52122.52125	142.142	"	"	"	
		00:30	360	10659	52122.52807	142.262	"	"	"	
		00:39	360	10662	52122.53460	142.377	"	"	"	
		00:46	360	10663	52122.53933	142.460	"	"	"	
		00:52	360	10664	52122.54398	142.543	"	"	"	
		01:00	360	10665	52122.54942	142.638	"	"	"	
		01:09	360	10667	52122.55512	142.739	"	"	"	
		01:16	360	10668	52122.56011	142.827	"	"	"	
		01:23	360	10669	52122.56498	142.913	"	"	"	
		01:30	360	10670	52122.57006	143.002	"	"	"	
		01:38	360	10672	52122.57538	143.096	"	"	"	
		01:45	360	10673	52122.58052	143.187	"	"	"	
		01:52	360	10674	52122.58564	143.277	"	"	"	
		02:00	360	10675	52122.59058	143.364	"	"	"	
		02:07	360	10676	52122.59541	143.450	"	"	"	
		02:15	360	10678	52122.60121	143.552	"	"	"	cloudy
		02:22	360	10679	52122.60602	143.637	"	"	"	cloudy

Table 1. (continued)

Date	Start UT	Exposure Time (s)	File ID	Mid BJD (2400000+)	Orbital Phase	Instr.	Spectral Range (Å)	Period	Comments	
Aug.	6	22:09	900	37106	52128.43328	246.432	Echelle	4327–6891	III	
		22:28	900	37107	52128.44668	246.669	"	"	"	
		22:46	600	37109	52128.45773	246.864	"	"	"	
		22:58	600	37110	52128.46569	247.004	"	"	"	
		23:09	600	37111	52128.47366	247.145	"	"	"	
		23:21	600	37112	52128.48182	247.289	"	"	"	
		23:35	600	37114	52128.49170	247.463	"	"	"	
		23:47	600	37115	52128.49971	247.604	"	"	"	
		23:58	600	37116	52128.50762	247.744	"	"	"	
		7	00:10	600	37117	52128.51557	247.884	"	"	"
			00:21	600	37118	52128.52348	248.024	"	"	"
			00:45	600	37121	52128.53984	248.312	"	"	"
			00:56	600	37122	52128.54783	248.453	"	"	"
		16	00:33	600	10729	52137.53196	406.937	B&C	3999–5188	IV
	00:44		1200	10730	52137.54310	407.134	"	"	"	
	01:07		1200	10732	52137.55883	407.411	"	"	"	
	23:26		1200	10740	52138.48867	423.814	"	3998–5187	"	
	23:48		1200	10742	52138.50420	424.088	"	"	"	
	17	00:11	1200	10744	52138.52008	424.368	"	"	"	
		00:35	1200	10746	52138.53647	424.657	"	"	"	
	27	22:19	1800	10993	52149.44533	617.095	"	3948–5136	V	
		23:00	1800	10995	52149.47395	617.600	"	"	"	
		23:37	1800	10997	52149.49919	618.045	"	"	"	
	28	00:53	1200	11003	52149.54910	618.925	"	5772–6976	"	
Sep.	5	22:16	2400	11021	52158.44629	775.876	"	3938–5125	VI	

Table 2. Peak separations (km s^{-1}) of emission lines averaged each day. The standard deviations are written in the parentheses. Each observing period is partitioned by horizontal lines.

JD*	He II 4686	H β	He II 5411	H α
52114	660 [†]		1320 [†]	740(40)
52116	1080(130)		1390 [†]	870(30)
52118	1050(150)			840(100)
52119	1020 [†]			
52121	1110(170)			
52122	1210(140)			1180(100)
52128	1260(230)	1250(210)		1060(90)
52137		1370(90)		
52138		1330(80)		
52149		1370(40)		1300 [†]
52158				

*JD–2400000.

[†]single spectrum. The typical $1\text{-}\sigma$ error for one measurement is $\sim 30 \text{ km s}^{-1}$.

complex, we measured the combined flux. The line flux of the C III/N III and He II lines became largest 4 days after the outburst maximum, while H α is almost constant. The C IV/N IV complex was seen only first three days.

Table 4 summarizes the daily averaged equivalent widths (EW) of other Balmer and He I absorption lines. Some of them became emissions later.

4.2. Period II (JD 2452119–2452122, 6th–9th day)

As in the period I, He II 4686, C III/N III Bowen blend, and H α were doubly-peaked emission lines (figure 4a). The fluxes of C III/N III, He II, and H α were smaller during the period II than those during the period I. The peak separation of He II 4686 was about same as that at the end of the period I. H α had peaks separated significantly broader than in the period I, and the peak separations of He II 4686 and H α were almost same.

The Balmer and He I absorption lines started to exhibit emission components in the wings (figure 4b). Table 4 shows that the EWs decreased, but these absorption feature became deeper between figures 3 and 4. The He II 4686 emission line suffered from significant contamination by He I 4713.

We have performed period analyses on the line flux of emission lines and the equivalent width of absorption lines obtained during this period, in the range of $10\text{--}100 \text{ d}^{-1}$. In these analyses, we used the data obtained in BJD

Table 3. Line fluxes in a unit of 10^{-12} erg cm $^{-2}$ s $^{-1}$ Å $^{-1}$ and equivalent widths in Å (a negative EW for an emission line) of emission lines averaged each day. The 1- σ errors are written in parentheses.

JD*	C III N III	He II [†] 4686	He II 5411	C IV N IV	H α
52114	7.2(0.9)	6.6(0.8)	1.6(0.2)	4.5(0.8)	2.6(0.3)
(EW)	-2.8(0.1)	-2.7(0.1)	-0.8(0.1)	-3.6(0.4)	-3.1(0.1)
52116	5.9(1.0)	6.7(1.0)	1.1(0.2)	2.7(0.3)	2.4(0.3)
(EW)	-3.8(0.3)	-4.0(0.2)	-0.8(0.1)	-3.3(0.1)	-3.2(0.1)
52118	7.7(1.5)	8.4(1.1)			2.4(1.0)
(EW)	-5.9(0.6)	-6.5(0.2)			-4.1(1.3)
52119 [‡]					
(EW)	-3.1(0.2)	-4.5(0.2)			
52121	1.8(0.5)	3.7(1.2)			
(EW)	-1.7(0.4)	-3.9(0.9)			
52122	2.8(0.6)	3.7(0.6)			1.1(0.3)
(EW)	-3.3(0.4)	-4.7(0.4)			-3.9(0.7)
52128	0.8(0.2)	2.6(0.5)			2.4(0.8)
(EW)	-1.2(0.2)	-4.7(0.5)			-8.2(2.0)
52137	1.0(0.2) [§]				
(EW)	-1.1(0.1) [§]				
52138	0.6(0.2) [§]				
(EW)	-0.8(0.1) [§]				
52149	-	-			0.5(0.1)
(EW)	-	-			-15.5(0.1)
52158	-	-			
(EW)	-	-			

*JD-2400000.

[†]Contaminated by the He I 4713 absorption line.

[‡]Flux was not able to be measured due to clouds.

[§]Combined flux of C III/N III and He II.

2452121.409–2452122.467 (July 30 and 31) for H δ , H γ , He I 4387, He I 4471, C III/N III, He II 4686, H β , and He I 4922, and the data obtained in HJD 2452122.506–2452122.607 (August 1) for He I 5875, H α , and He I 6678. The power spectra are exhibited in figure 5. Most of the lines seem to have modulated with periods close to P_{orb} . Confirmation is, however, needed, since the coverages are not quite sufficient. Note that Howell et al. (2003) also reported EW modulations of H and He with respect to the orbital phase in IR spectra obtained on 2001 July 27.

4.3. Period III (JD 2452128, 15th day)

The spectra were obtained with an echelle spectrograph in this period (figure 6). While the emission line fluxes of He II 4686 and C III/N III were smaller than those in the period II, that of H α became larger than in the period II (table 3). The intensities of the peaks of H α , especially the bluer peak, became much higher. The peak separations of He II 4686 and H α were 1260(\pm 230) km s $^{-1}$ and 1060(\pm 90) km s $^{-1}$, respectively (table 2).

As listed in table 4, He I absorption lines varied differently from a line to a line. He I 4388 became broader in EW, but He I 4471 was almost constant from the period I. He I 4922 and 6678 was in emission. The strong contamination from Na I makes it difficult to accurately measure

the equivalent width of He I 5875. The H β equivalent width became narrower, and the H α emission line grew in EW. The emission components of He I and Balmer lines got strong and the absorption components became deeper since from period II.

4.4. Period IV (JD 2452137-2452138, 24th-25th day)

This period corresponds to the very end of the main outburst. On the second day of this period, JD 2452138, WZ Sge was in the rapid fading phase. The averaged, normalized spectrum is drawn in figure 7. The spectra obtained on JD 2452137 show H γ and H δ emission components possibly superposed on shallow absorption features, while H β is a pure, strong, doubly-peaked emission line (table 4). All the Balmer lines were in pure emission on JD 2452138. He I 4387 and 4471 were in absorption, but He I 4921 was in emission with a doubly-peaked shape. The peak separations of H β were \sim 1350 km s $^{-1}$.

The C III/N III and He II 4686 emission lines had declined and was not able to be separated. They were, however, still present at the end of the main outburst.

4.5. Period V (JD 2452149, 36th day)

As stated above, WZ Sge repeated 12 short rebrightenings, after the main outburst. The observation of this

Table 4. Line fluxes in a unit of 10^{-12} erg cm $^{-2}$ s $^{-1}$ Å $^{-1}$ and equivalent widths in Å (a negative EW for an emission line) of absorption lines averaged each day.

JD*	He I 4026	H δ 4101	H γ 4340	He I 4388	He I 4471	H β 4861	He I 4922
52114	-3.3(0.3)	-12.4(2.0)	-11.1(1.1)	-0.6(0.2)	-4.8(0.3)	-7.4(0.2)	-1.0(0.2)
(EW)	1.0(0.1)	4.0(0.1)	4.0(0.1)	0.2(0.1)	1.8(0.1)	3.5(0.1)	0.5(0.1)
52116	-1.5(0.5)	-9.6(2.9)	-7.7(1.7)	-0.8(0.4)	-2.7(0.6)	-3.9(2.4)	-0.5(0.3)
(EW)	0.6(0.2)	4.0(1.2)	3.7(0.8)	0.4(0.2)	1.4(0.3)	2.5(1.5)	0.3(0.2)
52118	-1.2(0.4)	-5.8(2.5)	-4.4(1.4)	-0.7(0.2)	-2.4(0.8)	-2.2(1.3)	-0.6(0.3)
(EW)	0.6(0.2)	3.0(1.3)	2.6(0.8)	0.4(0.1)	1.5(0.5)	1.7(1.0)	0.5(0.2)
52119 \ddagger							
(EW)	0.5(0.1)	3.4(0.1)	3.1(0.1)	0.4(0.1)	1.6(0.1)	2.0(0.1)	0.5(0.1)
52121	-0.9(0.3)	-4.5(1.3)	-3.5(1.3)	-0.3(0.1)	-1.5(0.4)	-1.4(0.3)	-0.4(0.2)
(EW)	0.7(0.2)	3.5(1.0)	3.1(1.1)	0.3(0.1)	1.4(0.4)	1.7(0.4)	0.5(0.2)
52122		-3.1(0.5)	-2.9(0.4)	-0.4(0.2)	-1.6(0.3)	-1.3(0.2)	-0.5(0.2)
(EW)		2.6(0.4)	2.7(0.4)	0.4(0.2)	1.6(0.3)	1.6(0.2)	0.6(0.2)
52128				-1.0(0.3)	-1.1(0.3)	-0.6(0.6)	0.05(0.05)
(EW)				1.7(0.6)	1.9(0.5)	1.3(1.2)	-0.1(0.1)
52137	-0.08(0.03)	0.03(0.03)	-0.10(0.03)	0.05(0.02)	-0.1(0.1)	0.29(0.02)	0.13(0.02)
(EW)	0.3(0.1)	-0.1(0.1)	0.4(0.1)	-0.2(0.1)	0.5(0.4)	-1.5(0.1)	-0.7(0.1)
52138	-0.06(0.08)	0.27(0.15)	0.49(0.10)	0.09(0.03)	-0.03(0.05)	0.74(0.14)	0.11(0.07)
(EW)	0.3(0.4)	-1.4(0.8)	-2.9(0.6)	-0.5(0.2)	0.2(0.3)	-5.9(1.1)	-0.9(0.6)
42149			0.17(0.02)			0.25(0.03)	
(EW)			-3.4(0.4)	-	-	-6.2(0.8)	-0.1(0.1)
52158	0.09(0.04)	-0.57(0.03)	-0.53(0.10)		-0.13(0.01)	-0.27(0.03)	
(EW)	-0.7(0.3)	4.4(0.2)	4.4(0.8)	-	1.1(0.1)	2.8(0.3)	

*JD-2400000.

\dagger Contaminated by Na I D

\ddagger Flux was not able to be measured due to clouds.

JD	He I 5875 \dagger	He I 6678
52114	-1.0(0.1)	-0.2(0.1)
(EW)	0.9(0.1)	0.3(0.1)
52116	-0.3(0.1)	0.2(0.1)
(EW)	0.3(0.1)	-0.3(0.1)
52118	-0.8(0.3)	0.1(0.1)
(EW)	1.0(0.4)	-0.2(0.2)
52119		
(EW)		
52121		
(EW)		
52122	-0.7(0.2)	0.03(0.12)
(EW)	1.7(0.5)	-0.1(0.4)
52128	-0.5(0.2)	0.3(0.1)
(EW)	1.6(0.7)	-1.2(0.5)
52137		
(EW)		
52138		
(EW)		
52149	0.02(0.00)	
(EW)	-0.7(0.1)	
52158		
(EW)		

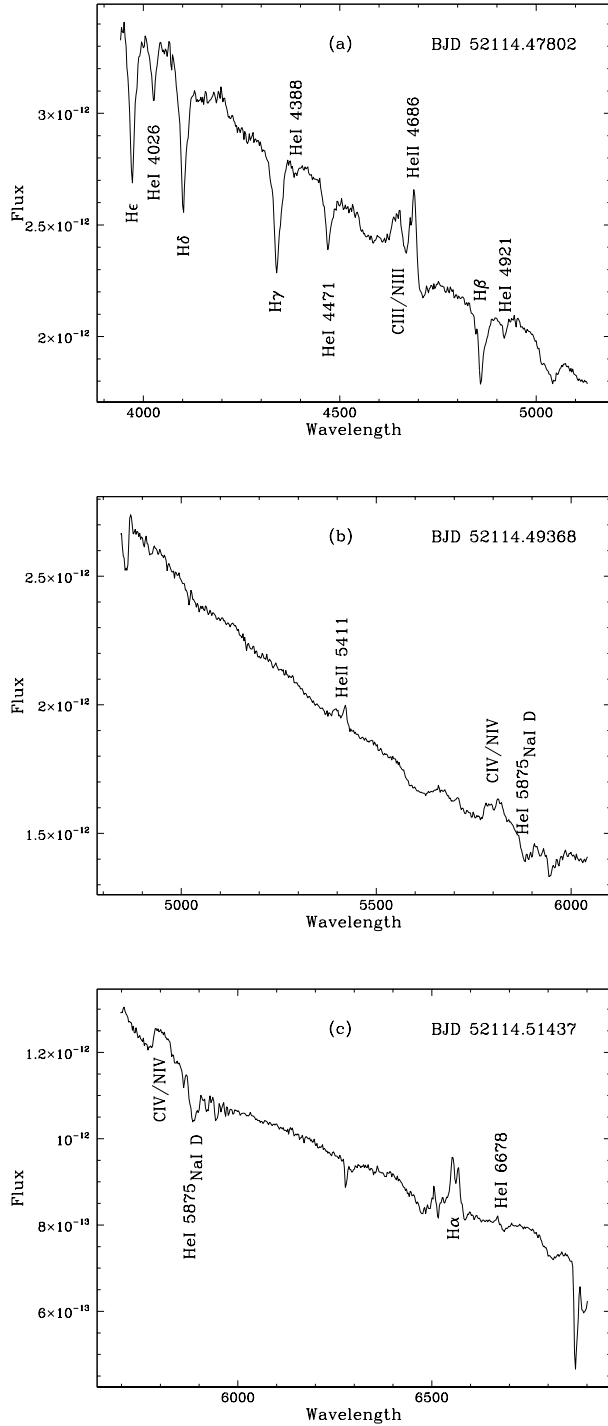


Fig. 2. Spectra (File ID: 10550, 10553, and 10558) around the maximum of the 2001 outburst of WZ Sge. The abscissa is the wavelength in \AA and the ordinate is the flux in $\text{erg cm}^{-2} \text{s}^{-1} \text{\AA}^{-1}$. The spectra have a very blue continuum and show Balmer, He I, and Na I D absorption lines, and He II, C III/N III Bowen blend, C IV and N IV emission lines.

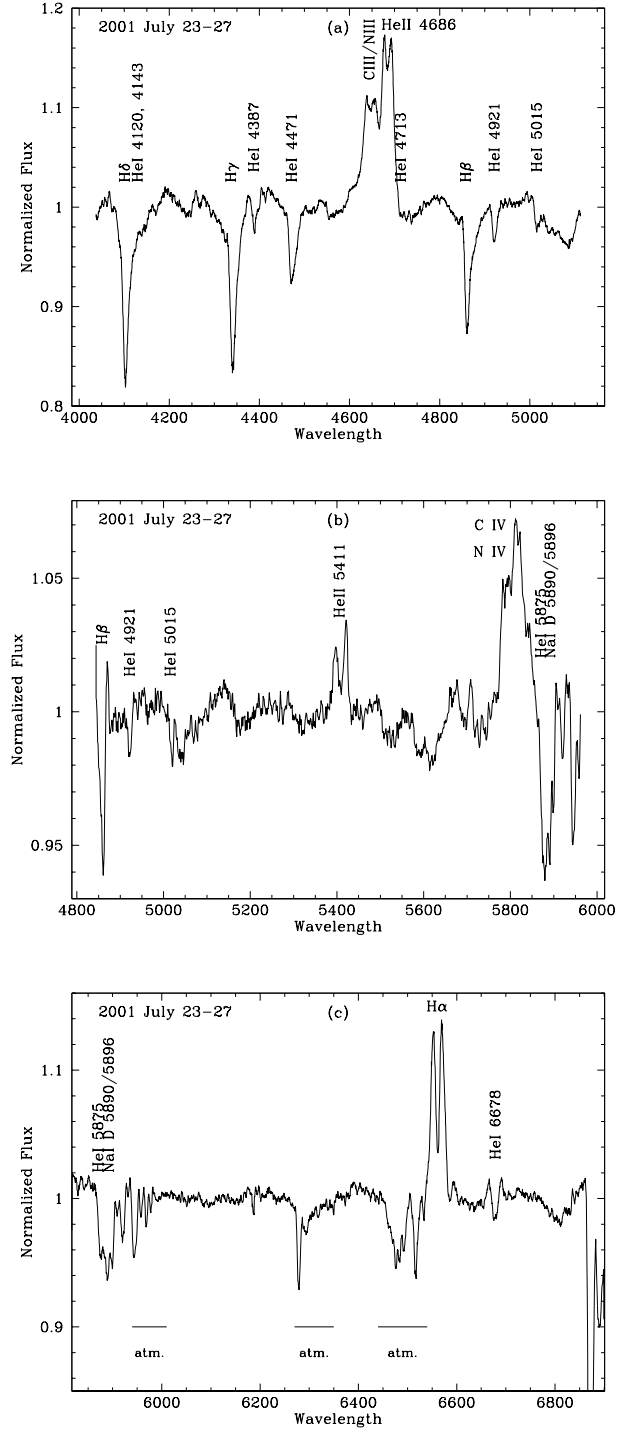


Fig. 3. Normalized spectra obtained by averaging the period I data of File ID: 10550–10603. Balmer, other than $H\alpha$, and He I lines are in absorption, and $H\alpha$ and He II emission lines have a doubly-peaked shape. Other high-excitation lines, i.e. C III/N III, C IV/N IV, are also present. The broad absorption feature around 5600\AA in Figure b and the broad and narrow troughs on the bluer side of $H\alpha$ in figure c are due to the atmospheric absorption.

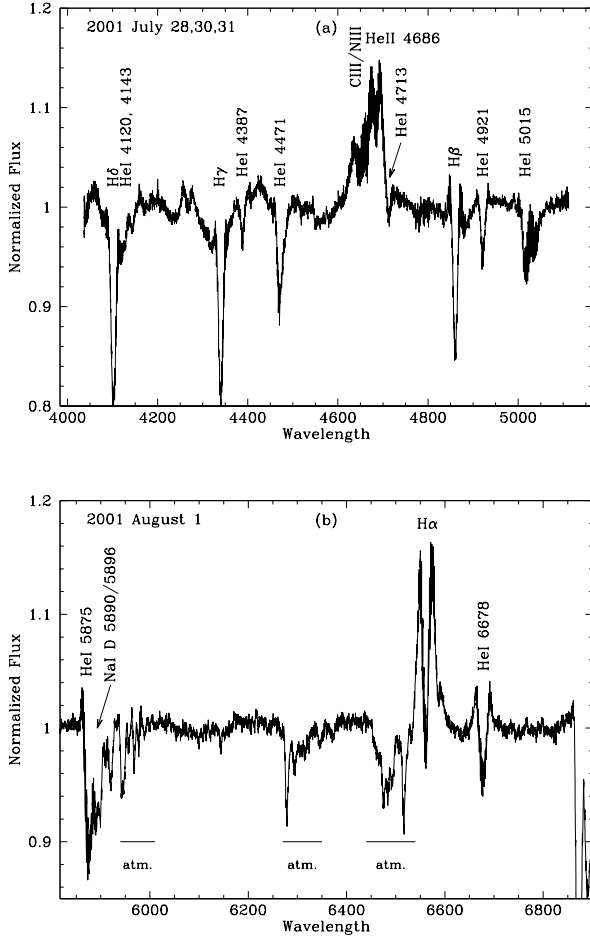


Fig. 4. Normalized spectra obtained by averaging the period II data of File ID: 10613–10679. Balmer, other than $H\alpha$, and He I lines are in absorption, while some of these lines exhibit emission components in the wing. $H\alpha$ and He II emission lines have a doubly-peaked shape, as in figure 3.

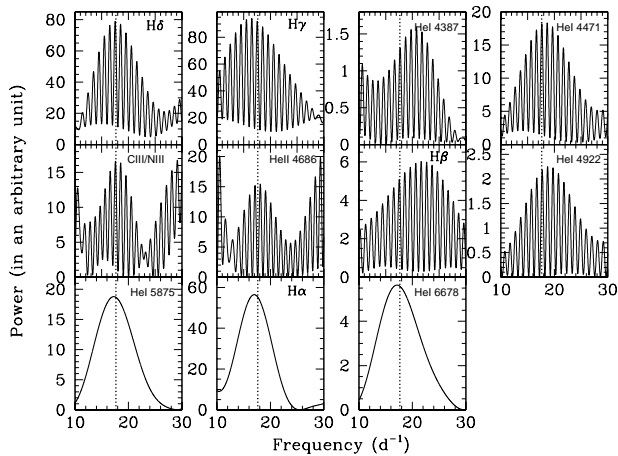


Fig. 5. Power spectra of the EW or line-flux variation in the period II. The dotted lines represent the orbital frequency. Most of lines seem to show modulations with periods close to P_{orb} .

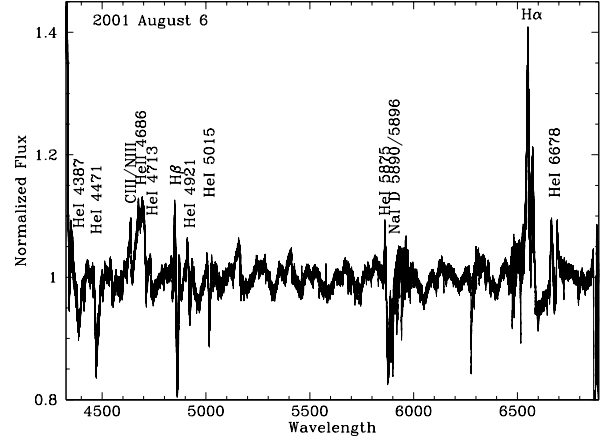


Fig. 6. Normalized spectra obtained by averaging the period III data of File ID: 37106–37122. The small ‘waves’ with a typical scale of ~ 130 Å are due to difficulty of complete sensitivity correction on echelle spectra.

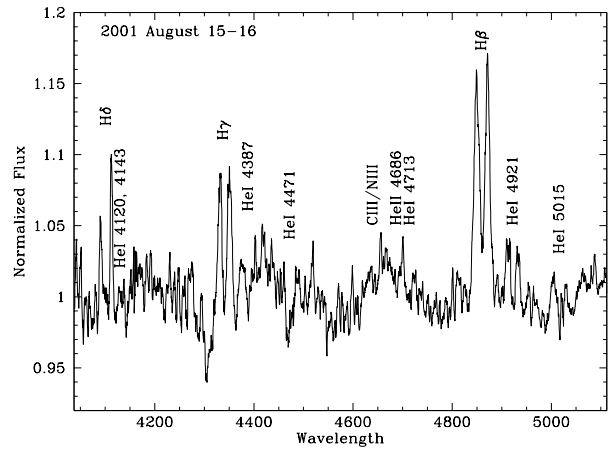


Fig. 7. Normalized spectrum obtained by averaging the period IV data of File ID: 10729–10746, at the end of the main outburst. Balmer lines became in strong emission. He I 4471 was a weak absorption, and He I 4921 was a weak doubly-peaked emission line. The He II 4686 and C III/N III emission lines had decreased, but were still clearly detectable.

period were carried out around the bottom of the dip between the third and fourth rebrightenings ($V \sim 12.4$). Spectral feature in figure 8a is almost identical with that in the period IV (figure 7). The He II 4686 and C III/N III emission lines, however, disappeared. In figure 8b, He I 5875 is a doubly-peaked emission line and the Na I D doublet which had been in deep absorption during the main outburst was not detectable. The peak separation of $H\alpha$ and $H\beta$ were ~ 1300 km s^{-1} and $1370(40)$ km s^{-1} , respectively. The red components of the doubly-peaked shapes in Balmer emission lines have stronger peak intensities than the blue components, while both components have almost same intensity in He I 5875.

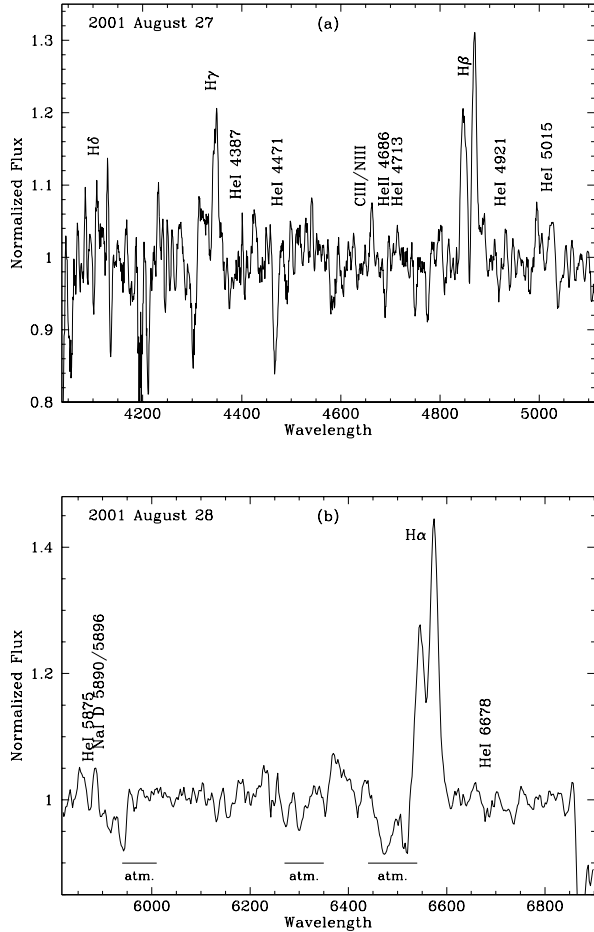


Fig. 8. Normalized spectrum obtained by averaging the period V data of File ID: 10993–10997, and normalized spectrum of File ID: 11003, which were obtained during the dip between the third and the fourth rebrightenings. Spectral feature in the upper panel was almost same as in figure 7. He II 4686 and C III/N III were not detectable. Na I D doublet observed during the main outburst disappeared.

4.6. Period VI (JD 2452158, 45th day)

Our last observation was performed around the top of the 9th rebrightening ($V \sim 11.7$). All the Balmer lines were in strong absorption (figure 9). These absorption lines have asymmetric shapes. The red slopes may be affected by an emission contribution. Note that the full width at zero intensity (FWZI) is broadest in H γ , and narrowest in H β among the Balmer lines. He I 4471 was still in strong absorption, but the other He I lines were weak. He II 4686 and C III/N III were not detectable, as well as in the period V.

5. Spectral Evolution

5.1. The 2001 outburst

The maximum time of this outburst can be accurately estimated to be BJD 2452114.7–2452114.8 with figure 1 in Ishioka et al. (2002). The first 6 low-resolution spec-

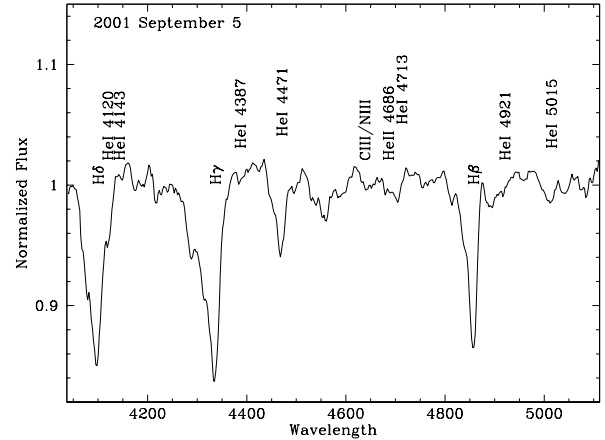


Fig. 9. Normalized spectrum of File ID: 11021. This spectrum was obtained at the 9th peak (period VI).

tra presented in Baba et al. (2002) were taken around HJD 2452114.26, about 12 hours before the maximum. The average spectrum of these contains only absorption lines of H α , H β , and He I 4922, 5876, and 6678. We performed the first run 5.5 hours after the observation by Baba et al. (2002), but still before the outburst maximum. As shown in figure 2 and 3, dramatic changes occurred on the spectrum in the meantime: H α became an emission line and high-excitation lines of C III/N III blend, He II 4686 and 5411, and surprisingly, C IV 5802/5813 and N IV 5786/5796 emerged. The C IV/N IV complex has been caught for the first time in the history of the dwarf nova study in the best knowledge of the authors. These C IV/N IV emission lines disappeared by the 5th day of the outburst (figure 4).

The emission lines of He II 4686, 5411 and C III/N III Bowen blend also emerged during 5.5 hours before our 1st run. In contrast to the C IV/N IV complex, these emission lines increased their line flux in period I, and persistently existed during the main outburst (table 3). Kuulkers et al. (2002) revealed existence of the spiral structure in the emissivity distribution of He II 4686 and the Bowen blend by the Doppler tomography technique (Marsh, Horne 1988) during the period I. Baba et al. (2002) also reported an asymmetric spiral structure of He II 4686 and no remarkable feature in the H α map.

The line flux of He II 4686 got larger for the period I, then decreased till JD 2452121. On the next day, He II 4686 rebrightened, and subsequently faded again. We did not detect this line during the rebrightening phase (period V and VI, figures 8 and 9). The C III/N III Bowen blend behaved in the almost same manner in the line flux.

The peak separation of He II 4686 was rather small, $\sim 660 \text{ km s}^{-1}$ on JD 2452114, then kept almost constant around 1100 km s^{-1} during the periods I and II. The small peak separation on the first day, which was as small as that of H α , may suggest that the surface temperature was very high ($\geq 25,000 \text{ K}$) even at the edge of the large accretion disk just before the outburst maximum (cf.

$\sim 1,400 \text{ km s}^{-1}$ of the peak separation of Balmer lines in quiescence, e.g. Mason et al. 2000). It is, however, noteworthy that this small value was measured in a spectrum of File ID 10550 obtained at an orbital phase of 0.255. The trailed spectra of He II 4686 in Baba et al. (2002) and Kuulkers et al. (2002) show that the peak separation varied with the orbital phase and was smallest at the phase around 0.25, although the peak separation might get broadened in the period of ~ 0.5 day between our first observation and that of Baba et al. (2002).

The He II 5411 already had a large separation of over $1,300 \text{ km s}^{-1}$ during the period I, which is as large as that of He II 4686 on JD 2452128. We can not see this line in the spectra in the period III (figure 6).

The Na I D absorption line was in deep absorption from the period I to, at least, the period III (figures 3, 4, 6), although it was not seen during the rebrightening phase (period V, figure 8).

At last, we describe the spectral evolution of Balmer lines. The spectra obtained by Baba et al. (2002) around BDJD 2452114.26 demonstrated $H\alpha$ and $H\beta$ in absorption. About 5.5 hours later, however, $H\alpha$ was observed to be a strong, doubly-peaked emission with a line flux of $2.6 \times 10^{-12} \text{ erg cm}^{-2} \text{ s}^{-1} \text{ \AA}^{-1}$, and an EW of -3.1 \AA (table 3). These values are about 30 times larger than that in quiescence in the line flux (Mason et al. 2000) and about 30 times narrower than that in quiescence in the EW (Gilliland et al. 1986). The peak separation was $740(40) \text{ km s}^{-1}$, half of that in quiescence. This fact suggests that the radius of the region forming the $H\alpha$ emission line was much larger just before the outburst maximum than that in quiescence. This topic will be discussed later (section 6.4). All the higher Balmer lines were in absorption in the period I (figure 3).

With the outburst going, the $H\alpha$ emission line steadily became strong in the EW, but stayed almost constant in the flux during the main outburst. The peak separation gradually grew. Nevertheless, it was about $1,100 \text{ km s}^{-1}$ in the period III, still smaller than that in quiescence. In the period V, i.e. in a minimum in the rebrightening phase, the flux of $H\alpha$ was smaller than that in the main outburst, but still several times larger than that in quiescence. The peak separation was significantly larger than that in the main outburst, but a little smaller than that in quiescence.

The other Balmer lines decreased their EWs with time, and then finally became emission lines in the period III ($H\beta$) and in the period IV ($H\gamma$ and $H\delta$), around the end of the main outburst. The $H\beta$ and higher Balmer lines were in absorption again in the period VI. The FWZIs of $H\gamma$ and $H\delta$ was much larger than those in the period I, making the EWs in the period VI broader than those in the period I.

5.2. Comparison with the spectra in other outbursts in WZ Sge

The spectra in the 15th, 17th, 19th, and 23rd day of the 1946 outburst observed by G. Herbig were reported by McLaughlin (1953). These spectra had doubly-peaked

emission lines of $H\beta$, $H\gamma$, and $H\delta$ with peak separations of $\sim 15 \text{ \AA}$ and FWZI of $\sim 50 \text{ \AA}$, in contrast to that $H\beta$ was in strong absorption with weak doubly-peaked emission component on the 15th day in the present outburst (period III, figure 6). The peak separations of $H\beta$ - $H\delta$ were ~ 500 - 800 km s^{-1} on the 15th day, much narrower than in the period III (section 4.3). Wide, weak absorptions of He I 4026 and 4471 were also present. They noted detection of Fe II 4233 and absorption features $-2,400 \text{ km s}^{-1}$ apart from $H\gamma$ and $H\delta$ and $-3,700 \text{ km s}^{-1}$ apart from $H\beta$, which were not in our spectra. On the other hand, McLaughlin (1953) mentioned that no other emission/absorption lines were found, though our spectra on the 15th day of the 2001 outburst (figure 6 and table 4) clearly show strong He II emission line.

The 1978 outburst was noticed at 1978 December 1.1 (UT) and reached its maximum on the same day (Patterson et al. 1978). The first spectroscopic observation was started at December 1.7 (UT) by Brosch et al. (1980). $H\alpha$ had a weak, singly-peaked profile in the spectra at December 1.7 (UT), but was observed to be in a doubly-peaked shape with peak separations of $\sim 500 \text{ km s}^{-1}$ in December 2.7-7.7. This constancy of the peak separation of $H\alpha$ was independently revealed by Gilliland, Kemper (1980). The velocities of the peaks of $H\alpha$ were also constant, within $\pm 15 \text{ km s}^{-1}$, on December 7 (Gilliland, Kemper 1980).

Crampton et al. (1979) also obtained optical time-resolved spectra on 1978 December 6 and 7. In their spectra, $H\beta$ was already in emission with double peaks (peak separation $\sim 600 \text{ km s}^{-1}$). The semi-amplitudes of the radial velocities of $H\beta$ were small, $19(\pm 7) \text{ km s}^{-1}$, $13(\pm 18) \text{ km s}^{-1}$, and $43(\pm 9) \text{ km s}^{-1}$ for the central absorption, the blue peak, and the red peak, respectively. The average semi-amplitude of those radial velocities of $H\gamma$ - δ was larger, $162(\pm 37) \text{ km s}^{-1}$. C III/N III emission was already weak at that time.

Patterson et al. (1978) reported on spectral lines in their time-resolved spectra. Although the date when the spectra were taken is not written in the IAU Circular, the line feature of the Balmer series, He I, He II, and the Bowen blend is nearly identical with ours in the period I and II. The spectra in the early phase obtained by Ortolani et al. (1980) also showed the same feature.

Nevertheless, the variation of the lines in the later phase in the main outburst (Gilliland, Kemper 1980; Ortolani et al. 1980; Walker, Bell 1980) was different from that in our spectra: He II 4686 was already weak on the 10th day, and $H\alpha$ became weaker in contrast to that it became stronger in our data (table 3).

In the dip and the rebrightening phase, the spectra in Ortolani et al. (1980) was again the same as ours.

As seen in this section, the spectral feature and its evolution seem slightly different among those in the 1946, 1978, and 2001 outbursts, even in the same system WZ Sge.

5.3. Comparison with the spectra in other SU UMa stars in superoutburst

The spectroscopic observations of an eclipsing dwarf nova, Z Cha in superoutburst were done by Vogt (1982) and Honey et al. (1988). Doubly-peaked emission lines of the Balmer series superposed on shallow, broad absorption components, He I absorptions, and emission lines of He II 4686 and C III/N III were seen in their spectra. Wu et al. (2001) spectroscopically observed another eclipsing star, IY UMa during the 2001 superoutburst. They also observed emission lines of the Balmer series, He I, and the He II-C III/N III complex. In addition, Na I D absorption was detected.

In contrast to the high-inclination systems including WZ Sge in this paper, VY Aqr (Augusteijn 1994) and SX LMi (Wagner et al. 1998) in superoutburst did not have the emission line of He II 4686. Another WZ Sge star, EG Cnc did not show the He II 4686 emission line (Patterson et al. 1998a). Their spectra of EG Cnc were, however, obtained during the rebrightening (echo-outburst) phase, and this emission line was not firmly detected also in our spectra in the rebrightening phase (phases V and VI, figures 8 and 9). Na I D absorption was seen in the EG Cnc spectra, while we can not see it in the rebrightening phase (figure 8).

The spectra of another WZ Sge star, V592 Her obtained on the 3rd day of the outburst by Mennickent et al. (2002) showed absorption lines with an emission core of the Balmer series including H α and He I, and a weak doubly-peaked emission line of He II 4686. Na I absorption was not present in the spectra.

In conclusion, visibility of the He II 4686 emission line seems to depend on the inclination, and it is not only in WZ Sge-type dwarf novae that the Na I D line is seen.

6. Discussion

6.1. Outburst properties

The outbursts in WZ Sge had been observed three times in 1913, 1946, and 1978 with a recurrence cycle of 32.5 years. Breaking this punctuality, however, WZ Sge has underwent a new outburst *only* 23 years after the last 1978 outburst.

Besides of the stable recurrence cycle of the first three outbursts, the long term outburst light curve varied from one to the other (see figure 1 in Kuulkers et al. 2002; see also figure 1 in Ortolani et al. 1980). In the 1913 outburst, the main outburst seems to have lasted about 38 days, or maybe had lasted around 28 days and the point on the 37th day from the onset was in the rebrightening phase (see Brosch 1979; Ortolani et al. 1980). The 1946 outburst consists of only a main outburst of 29 days followed by a long fading tail (Mayall 1946; Eskioglu 1963). During the 1978 outburst, the best observed one among these three, WZ Sge had kept the plateau phase of the main outburst for 32 days. After a dip of ~ 3 days following the plateau phase, WZ Sge caused a rebrightening which lasted at least 20 days. It is not clear whether

this rebrightening was the ‘second superoutburst’ as in the AL Com 1995 outburst (Nogami et al. 1997a), or a complex of many repetitive outbursts like during the current outburst. Comparing these previous outbursts, the 2002 outburst has characteristics of the relatively short main outburst of ~ 25 days and the following rebrightening phase consisting of 12 short outbursts for 24 days.

The total energy emitted during the 1978 outburst seems a little larger than that during the 2001 outburst, at least, if we compare them in optical. The ratio of them is, however, obviously smaller than the ratio of the quiescence durations before each outburst, i.e. 33 years to 23 years. Regarding the 1946 outburst and the 1978 one, the outburst light curves indicate that the radiated energy during the 1946 outburst was much smaller than that during the 1978 outburst, while the quiescence durations before each outburst were nearly the same, ~ 33 years. These imply that the condition to cause an outburst in WZ Sge does not depend only on the mass stored in the accretion disk, and the mass transfer changes even in WZ Sge (an increasing trend at least in these several tens of years).

Variations of the outburst patters have been minutely demonstrated in many dwarf novae, especially in recent years, such as in DI UMa (Fried et al. 1999), SU UMa (Rosenzweig et al. 2000; Kato 2002b), V1113 Cyg (Kato 2001), V503 Cyg (Kato et al. 2002), DM Lyr (Nogami et al. 2003a) and MN Dra (Nogami et al. 2003b). The currently most plausible model for these variations is rooted in the the solar-type cycle in the secondary star (Warner 1988; Bianchini 1990; Ak et al. 2001). If this scenario is true, the secondary star in WZ Sge is suggested to have magnetic activities, although the secondary is considered to be (close to) a degenerate star as described above.

This would be observed as changes of the brightness in quiescence. Although analyses of the quiescent eclipse times and the long-term light curve of WZ Sge by Skidmore et al. (2004) have yielded no evidence for cyclical modulations, it will be necessary to pile up the quiescence observations for more decades in order to judge the magnetic activity of the secondary star. The continuous observation reports by amateur observers will be of much help for this study.

6.2. Radial Velocity Variations and Line Forming Regions

During the previous 1978 outburst, Gilliland, Kemper (1980) found that the radial velocities of the emission components of H α stayed constant within ± 15 km s $^{-1}$ and the peak separation of this line (~ 440 km s $^{-1}$) did not vary for over one orbital period in the spectra obtained in the 7th night of the outburst. This separation did not change from the 5th night to the 8th night.

Our observations, however, do not affirm the stationary H α emission. The H α peak separation indicated an increase trend (table 2), and the radial velocity changed with a large amplitude. Table 5 summarizes the radial

Table 5. Radial velocities of lines in a unit of km s^{-1} on 2001 July 30 and 31, and August 1 and 6. The marks, * and † represent the blue component and the red component of the double peaks, respectively. The typical $1\text{-}\sigma$ error is $\sim 30 \text{ km s}^{-1}$.

July 30 Frame ID	H ϵ	He II 4026	H δ	H γ	He I 4471	He II* 4686	He II† 4686	H β	He I 4921	He I 5015
10616	-6.9	-44.0	-43.9	-58.8	-88.2	-855.3	582.9	-52.0	-58.1	126.2
10618	161.3	257.6	47.7	-15.6	63.9	-469.8	614.1	-3.7	97.9	153.8
10620	154.7	130.2	6.8	-10.9	37.5	-578.4	590.0	-49.8	50.5	68.7
10622	75.3	119.8	-49.6	-88.8	-120.8	-467.5	482.2	-90.8	-59.8	150.1
10624	-19.5	47.7	-94.8	-118.5	-96.2	-865.8	312.5	-132.1	-107.0	34.2
10625	-21.4	28.1	-112.7	-142.1	-99.6	-546.8	464.0	-154.5	-47.9	28.3
10626	-12.5	-24.2	-78.8	-159.1	-119.6	-568.1	453.2	-137.3	-70.6	-102.7
10628	47.8	-19.8	-90.5	-86.3	-158.2	-859.1	474.9	-62.2	-185.9	-87.1
10629	125.4	209.2	49.0	-53.6	-9.7	-570.5	486.9	-44.0	-18.2	105.9
10630	276.7		185.9	145.6	185.0	-344.5	577.2	106.1	97.7	351.6
10631	455.7	404.1	280.8	259.0	292.6	-293.8		234.7	360.8	415.5

July 31 Frame ID	H δ	H γ	He I 4471	He II* 4686	He II† 4686	H β	He I 4921	He I 5015
10637	-6.4	-105.5	-76.0	-852.3	513.4	-110.8	-49.6	-91.4
10639	-86.4	-115.7	-165.6	-841.6	250.9	-115.0	-130.2	-172.0
10640	-11.5	-64.6	-14.0	-753.4	469.5	-73.4	-31.0	-7.0
10642	179.2	79.3	99.8	-432.2		73.6	135.3	90.9
10644	257.1	177.5	282.2	-807.4	449.4	171.9	174.4	270.0
10645	83.7	40.3	94.3	-752.6	673.0	20.8	-41.9	67.1
10646	79.5	-20.2	-32.7	-543.7	501.7	-9.2	-4.0	105.9
10648	-57.5	-111.0	-122.0	-678.1	358.0	-137.1	-77.6	-43.3
10649	-128.0	-175.8	-176.9	-829.3	376.0	-168.7	-127.7	-151.8
10650	-82.4	-108.1	-178.1	-819.0	438.3	-119.0	-139.4	-131.7

August 1 Frame ID	He I 5875	H α *	H α †	He I 6678
10654	175.8	-521.2	652.8	187.3
10656	116.6	-670.3	520.3	108.8
10657	129.9	-633.5	599.9	70.1
10658	-20.9	-616.8	549.4	-26.7
10659	-72.9	-618.8	369.6	-83.8
10662	-67.2	-730.5	493.9	-129.7
10663	14.1	-826.7	565.5	-117.7
10664	-5.7	-700.7	494.7	-6.5
10665	20.8	-590.1	500.6	-45.7
10667	136.3	-508.5	539.0	54.0
10668	251.4	-496.0	674.4	190.7
10669	142.3	-510.7	663.2	131.7
10670	-39.5	-636.6	670.7	45.5
10672	28.8	-656.1	590.3	-15.4
10673	-33.5	-627.4	413.5	-37.9
10674	-49.4	-637.4	479.0	-68.5
10675	-69.5	-598.7	556.0	-131.5
10676	-85.4	-714.8	574.2	-118.1
10678	34.5	-695.1	555.3	69.7
10679	27.1	-607.9	517.7	52.8

Table 5. (continued)

August 6 Frame ID	He I 4387	He I 4471	He II* 4686	He II [†] 4686	H β * 4686	H β [†] 4686	He I* 4921	He I [†] 4921	He I 5015	He I 5875
37106	-88.6	-4.7	-732.8	426.0	-739.8	633.6	-728.2	675.7	20.7	33.3
37107	118.7	105.9	-507.7	509.4	-578.5	647.8	-572.6	724.3	116.7	99.6
37109	-63.5	335.0			-501.9				264.4	381.9
37110	142.7	326.7	-650.8	981.4	-686.9		-624.5	973.8	88.6	345.3
37111	17.6	78.8		478.4	-695.7		-659.5		82.4	46.0
37112	-44.7	-35.1			-707.6		-698.4		54.8	-36.8
37114	-27.1	19.5	-707.3	344.3	-747.5	637.7	-749.6	704.3	39.3	20.3
37115	45.4	67.1	-713.6	1062.3	-687.1	638.1	-635.7	713.1	81.9	87.4
37116	209.6	189.9	-470.2	675.3	-533.3	817.1	-512.9	789.6	185.4	205.5
37117	291.4	296.9			-594.6	263.3	-644.6	1131.3	273.0	293.7
37118	157.8	169.8	-590.1	877.8	-654.1	263.3	-607.9	956.5	82.2	321.2
37121	-57.5	-107.1			-763.0	645.1	-726.7	861.0	6.8	-69.5
37122	-20.9	6.2	-784.8	584.1	-789.6	607.6	-751.5	682.9	41.8	30.5

August 6 Frame ID	H α * 4686	H α [†] 4686	He I* 6678	He I [†] 6678
37106	-678.3	458.9	-660.5	633.5
37107	-565.6	480.7	-581.1	628.2
37109			-450.9	743.1
37110			-631.1	766.8
37111	-625.5	420.0	-650.3	549.7
37112	-615.4	269.0	-670.2	614.9
37114	-673.6	460.3	-687.1	624.8
37115	-636.6	481.5	-661.8	611.7
37116	-528.1	523.1	-498.9	632.7
37117	-509.2			
37118	-621.5		-601.1	
37121	-652.1	305.3	-697.2	618.5
37122	-717.7	463.6	-704.8	586.4

velocities of each emission/absorption lines measured by fitting a Gaussian function during the periods II and III. Table 6 lists the parameters of the semi-amplitude (K), the red-to-violet crossing time (T'_0), the corresponding phase offset (ϕ_0) and the systemic velocity γ obtained by sinusoid fitting using the known orbital period. The radial velocities in table 5 and the sinusoids with parameters in table 6 are shown in figure 10.

Most of the phase offsets are within the range of $\phi_0 = 0.08 - 0.13$, with exceptions being those of the H β red peak, the red peak of He I 4921, the H α red peak on August 6. This phase shift of $\phi_0 \sim 0.11$ may be against a hypothesis that the lines originate from the accretion disk. A shift of an almost same value was, however, also observed in quiescence, which was interpreted to be due to an effect by the hotspot contribution (Mason et al. 2000). In the present case, the spiral structures in the disk possibly have a stronger effect (see Baba et al. 2002; Kuulkers et al. 2002). Then, the possibility is not rejected that the lines were formed on the accretion disk.

The reason for the unusual phase offsets of the red peaks of H β , He I 4921, H α is left as an open problem. Confirmation of this phenomenon is desired during future

outbursts.

The semi-amplitudes are larger than those in quiescence, except for $\sim 75 \text{ km s}^{-1}$ of H α consistent with $68(\pm 3) \text{ km s}^{-1}$ in quiescence (Mason et al. 2000), which probably suffer from contamination of the spiral arms, too.

The absorption line of Na I D definitely existed in our first spectrum, though it is not clear in figure 2 because of the contamination of He I 5875. As previously mentioned, this absorption line was found in IY UMa (Wu et al. 2001) and EG Cnc (Patterson et al. 1998a) in outburst. Patterson et al. (1998a) interpreted that an extensive cool region in the disk is an origin of Na I absorption, based on the broad FWZI. Although the contamination of the He I absorption obstructs a measurement of the FWZI of Na I D in our spectra, we can estimate the relative radial velocity using the profile from the bottom of the absorption to the red wing. The estimates in this way set limits on the semi-amplitude of the radial velocity variation to be smaller than 25 km s^{-1} , which is smaller than that of the white dwarf (see Steeghs et al. 2001a). Thus, the origin of the absorption is suspected to be a rather stationary region, such as the center of mass of this system, or the part of the disk extended over the secondary star

(see section 6.4). It deserves attention that the absorption depth reaches 0.08 in the normalized intensity (figure 4).

6.3. Emission lines and the outburst mechanism

The first spectra (ID: 10550) of our data was obtained at BJD 2452114.48 (table 1), which is several hours before the outburst maximum. He II 4686 was a doubly-peaked emission line with a peak separation of $\sim 660 \text{ km s}^{-1}$ in this spectrum obtained at $\phi = 0.255$. The spectrum (ID: 10557) obtained one hour after, but still before the maximum, showed H α emission line with double peaks of a $\sim 780 \text{ km s}^{-1}$ separation. These small separations mean that the accretion disk was greatly extended before the outburst maximum (see the next section). This qualitatively agrees with the prediction on the outside-in type outburst due to the disk instability (see e.g. Ichikawa et al. 1993).

The spectra obtained by Baba et al. (2002) by 5.5 hours before our first observation contain only absorption lines of the Balmer series including H α and He I and no hint of emission lines of highly ionized species: He II 4686, C III/N III. It should be a natural scenario that the innermost part of the accretion disk and the white dwarf was fully heated up by the accreted mass, and irradiation by this region formed a temperature-inversion layer (chromosphere) on the disk during this interval of 5 hours, then the chromosphere produced these high-excitation emission lines.

The C IV/N IV emission lines, which was observed on the 1st and 3rd days of this outburst, do not bear a clearly doubly-peaked shape. On JD 2452114, the FWZI of this blend line is very broad, 4000–5000 km s^{-1} , which is comparable of $\sim 5600 \text{ km s}^{-1}$ of the combined line of the C III/N III blend and He II 4686. However, the FWZI of C IV/N IV is much broader than that of H α (2200 km s^{-1}), even taking into account the separation of the blended lines. These two facts (the non-doubly-peaked profile and the broad FWZI) imply that the C IV and N IV lines originated in the boundary layer between the accretion disk and the white-dwarf surface, or in the very inner region of the accretion disk.

On the other hand, there still remains a possibility that the C IV/N IV complex was formed in the chromosphere in the accretion disk, like He II 4686. Our instruments may not have a resolution power to resolve their doubly-peaked profiles. Higher spectral-resolution (and time-resolved) spectroscopy from the initial phase of the future outbursts are encouraged.

These evolution courses of the high-excitation lines are also reasonably understandable within the outside-in outburst scheme of the disk instability. The C IV/N IV emission line weakened from the 1st day to the 3rd day, and disappeared by the 5th day of the outburst, indicating that the temperature of the very inner side of the accretion disk started decreasing at the near-the-maximum phase of the outburst. However, He II 4686 was present throughout the main outburst. It will be a challenge for the disk instability model to reproduce the variation of the temperature and density structure in the accretion

Table 6. Fitted semi-amplitudes (km s^{-1}), T_0 (BJD – 2452120), systemic velocities (km s^{-1}) of lines on 2001 July 30 and 31, and August 1 and 6. The marks, * and † represent the blue component and the red component of the double peaks, respectively.

July 30				
Line	K	T_0	ϕ_0	γ
He ϵ	210(31)	1.442(1)	0.10(2)	131(20)
He II 4026	200(43)	1.442(2)	0.10(4)	145(27)
H δ	170(29)	1.441(1)	0.09(2)	19(19)
H γ	170(33)	1.441(1)	0.09(2)	17(21)
He I 4471	192(38)	1.442(1)	0.10(2)	5(25)
He II 4686*	208(85)	1.443(3)	0.12(5)	–557(54)
He II 4686†	76(32)	1.441(3)	0.09(5)	533(20)
H β	151(29)	1.440(2)	0.07(5)	–28(19)
He I 4921	181(49)	1.442(2)	0.10(4)	24(31)
He I 5015	195(55)	1.442(2)	0.10(4)	133(35)
July 31				
Line	K	T_0	ϕ_0	γ
H δ	157(23)	2.463(1)	0.11(2)	55(17)
H γ	143(15)	2.463(1)	0.11(2)	–11(11)
He I 4471	191(26)	2.463(1)	0.11(2)	10(19)
He II 4686*	78(66)	2.463(8)	0.11(14)	–714(48)
He II 4686†	106(44)	2.467(5)	0.18(9)	473(36)
H β	140(16)	2.463(1)	0.11(2)	–18(12)
He I 4921	122(30)	2.462(2)	0.10(2)	–4(22)
He I 5015	175(27)	2.464(1)	0.13(2)	30(20)
August 1				
Line	K	T_0	ϕ_0	γ
He I 5875	117(17)	2.575(1)	0.09(2)	39(12)
H α *	78(20)	2.576(2)	0.11(4)	–636(14)
H α †	72(21)	2.575(2)	0.09(4)	553(15)
He I 6678	130(14)	2.576(1)	0.11(2)	14(10)
August 6				
Line	K	T_0	ϕ_0	γ
He I 4387	113(36)	8.471(3)	0.10(5)	56(25)
He I 4471	171(22)	8.473(1)	0.13(2)	118(15)
He II 4686*	158(40)	8.468(1)	0.05(2)	–654(26)
He II 4686†	259(126)	8.472(5)	0.12(9)	676(81)
H β *	107(19)	8.469(2)	0.06(4)	–666(13)
H β †	217(86)	8.454(3)	–0.20(5)	499(50)
He I 4921*	88(19)	8.470(2)	0.08(4)	–650(13)
He I 4921†	174(42)	8.480(2)	0.26(4)	854(25)
He I 5015	98(19)	8.470(2)	0.08(4)	105(13)
He I 5875	182(27)	8.473(2)	0.13(4)	143(18)
H α *	73(18)	8.472(2)	0.12(4)	–606(12)
H α †	89(33)	8.463(5)	–0.04(9)	432(27)
He I 6678*	94(19)	8.470(2)	0.08(4)	–615(13)
He I 6678†	55(27)	8.474(5)	0.15(9)	649(17)

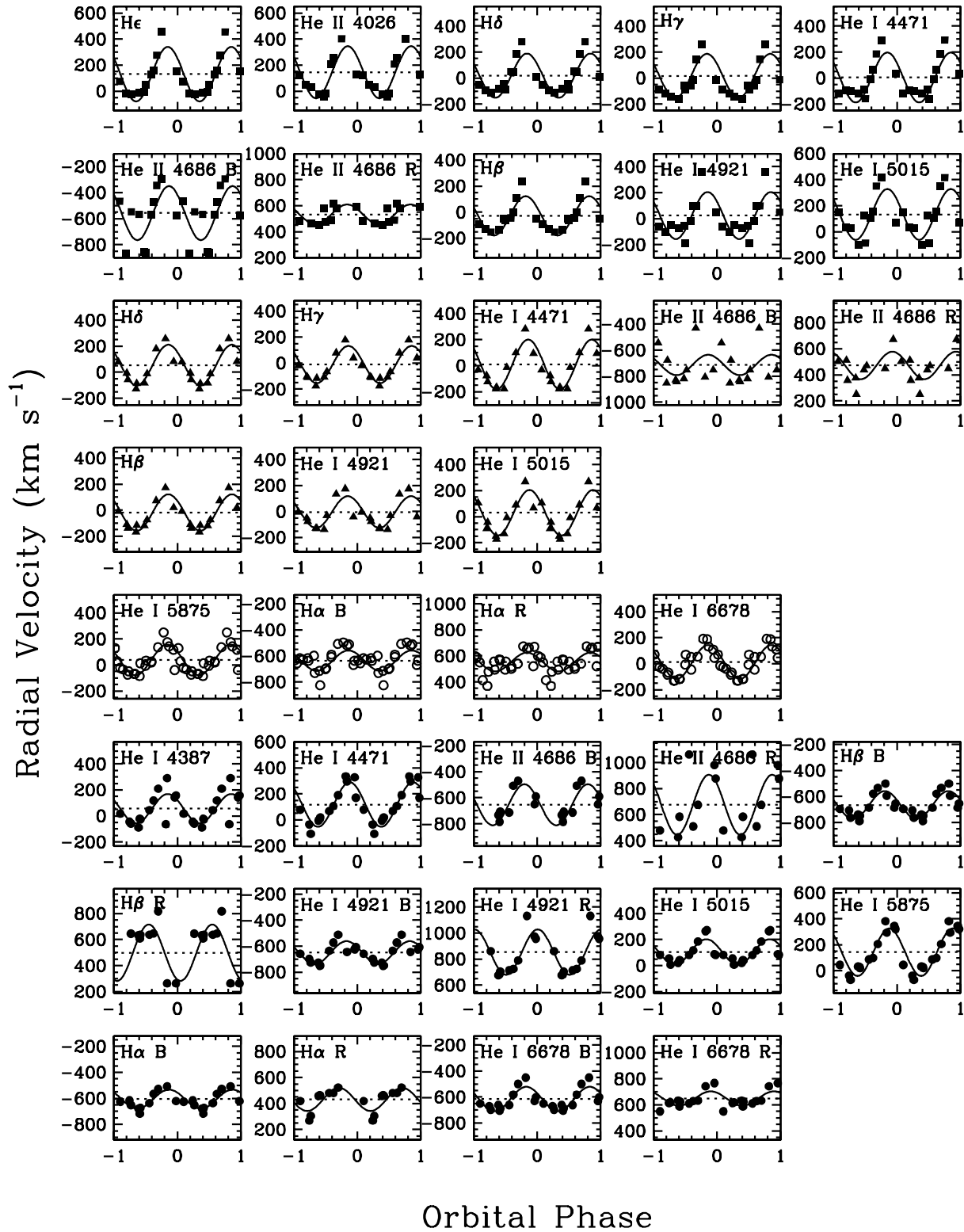


Fig. 10. Radial velocities of emission/absorption lines of July 30 and 31, and August 1 and 6. The marks represents the data in table 5, and the sine curves (table 6) obtained by fitting the RVs are drawn in each figure. The figures in the top 2 rows (filled square), the third and fourth rows (filled triangle), the fifth row (open circle), and the bottom 3 rows (filled circle) displays RVs measured on 2001 July 30 and 31, and August 1 and 6, respectively.

disk which can produce the spectral evolution of these high-excitation lines in the special case of WZ Sge.

6.4. Maximum disk radius

The peak separation is generally regarded to be indicative of the velocity at the outer edge of the accretion disk multiplied by $\sin i$, where i is the inclination angle. The separation of $H\alpha$ was $740(40) \text{ km s}^{-1}$ on JD 2452114 (table 2), which was about a half of 1450 km s^{-1} in quiescence (Skidmore et al. 2000). If we assume the Keplerian circular velocity and the disk radius $r_{\text{disk}} = 0.3a$ (a : the binary separation) in quiescence (Robinson et al. 1978), then the radius at the maximum of the outburst is suggested to exceed the binary separation ($r_{\text{disk}} \sim 1.2a$). Such a circumstellar disk was first introduced by Gilliland, Kemper (1980) to explain the narrow peak separation ($\sim 440 \text{ km s}^{-1}$) of stationary $H\alpha$ observed during the 1978 outburst of WZ Sge (see also Brosch et al. 1980; Friedjung 1981). The Na I D absorption line may be formed in the circumbinary part of this extended disk, though this hypothesis requires a significant contribution of that part to the continuum light to produce the absorption depth of 0.08.

To create a circumstellar disk, the outer edge of the disk must extend over the critical radii of the 2:1 resonance and the tidal truncation, and the Roche lobe. Leibowitz, Mazeh (1981) proposed a model to create the external disk, or ring, that the radiation pressure at the outburst may make gases pour out from the L2 point. There has been, however, no observational evidence for the mass flow via the L2 point.

Here, we should pay attention to the following two points: 1) the peak separation on JD 2452114 was determined using only the two spectra obtained at $\phi = 0.847$ (ID: 10557) and $\phi = 0.896$ (ID: 10558), and 2) we assumed the Keplerian velocity. As for the first point, the peak separation observed in a spectrum changes under the influence by the variations of the emission profile, as mentioned above. The separation was, however, derived from the spectra obtained at different orbital phases on JD 2452116 and 2452118 (table 1), and maintained small values ($< 900 \text{ km s}^{-1}$) by JD 2452118 (table 2). If we take the 900 km s^{-1} separation, the resultant radius of $r_{\text{disk}} \sim 0.77a$ still exceeds the theoretical maximum radius and the critical radius of the 2:1 resonance (Osaki, Meyer 2003).

The second point arises from a question whether the Keplerian velocity law holds up to the outer edge of the outbursting disk, especially around the outburst maximum. For this problem, Osaki, Meyer (2003) used the value of $1,000 \text{ km s}^{-1}$ in the discussion of the maximum disk radius, based on the Doppler maps of He II and $H\alpha$ in Baba et al. (2002), although these maps seem to admit a choice of a larger separation.

To discuss more about this topic, we need higher spectral- and temporal-resolution spectroscopy around the outburst maximum, detailed theoretical works and simulations on the behavior of the outbursting accretion disk.

6.5. Alternation between the early/genuine superhump

According to Patterson et al. (2002) and Ishioka et al. (2004), the genuine superhumps emerged on JD 2452126. The period I and II are characterized by the early superhumps, and the genuine superhump were observed during the period III and later.

Figure 11 displays the typical variations of the emission-line profiles of $H\alpha$ in the periods II and III, and of $H\beta$ in the period V in an orbital period. The V/R ratio of the peaks of $H\alpha$ varied around 1 in period II when we saw early superhumps. In contrast, one of the peaks was stronger through the orbital phase in the periods III and V, when genuine superhumps were prominent. This clearly proves the different nature between the early superhump and the genuine superhump.

Interchange of the stronger peak with a beat period of the superhump period and the orbital period has been interpreted to be evidence of the precessing eccentric disk (Vogt 1982; Hessman et al. 1992; Augusteijn 1994; Wu et al. 2001). The current plausible models for the early superhump phenomenon are the tidal dissipation model (Osaki, Meyer 2002) and the tidal distortion model (Kato 2002a). The present data indicate that the disk was not yet eccentric on JD 2452112 (section 6.2), the 10th day of the outburst and 4 days before the genuine superhump emergence. To test these model, it may be a key to examine which model can more naturally allow a sudden change of the disk structure which was observed photometrically (Patterson et al. 2002; Ishioka et al. 2004) and spectroscopically (this work).

6.6. Rebrightening phase

The periods V and VI are around the third minimum and at the ninth peak during the rebrightening phase, respectively. All the Balmer lines and He I except for He I 4471 are doubly-peaked emission lines during the period V (figure 8), as in quiescence (see e.g. Downes, Margon 1981), although the broad absorption component of the white dwarf is not seen around any Balmer emissions. During the period VI (figure 9), the Balmer lines were basically in absorption, although they seem to have weak emission components of doubly-peaked shapes at the same time. This change of the hydrogen and helium absorption lines to emission lines with a change from a faint state to a bright state means that propagation of the heating/cooling wave gave rise to the state transition, as in the normal outburst of dwarf novae (see Osaki et al. 2001).

The peak separations of the Balmer lines in table 2 were slightly narrower than those in quiescence, indicating that the accretion disk had already shrunk to be $\sim 0.37a$, close to that in quiescence, and was well within the critical radius of the 3:1 resonance ($0.46a$). The eccentricity of the disk is, however, still maintained, as indicated by the persistently strong red peak of $H\alpha$ in the period V (see the previous section) and the asymmetric profile of absorption lines in the period VI.

The high-excitation emission lines of He II 4686 and C III/N III, of course also C IV and N IV, are neither de-

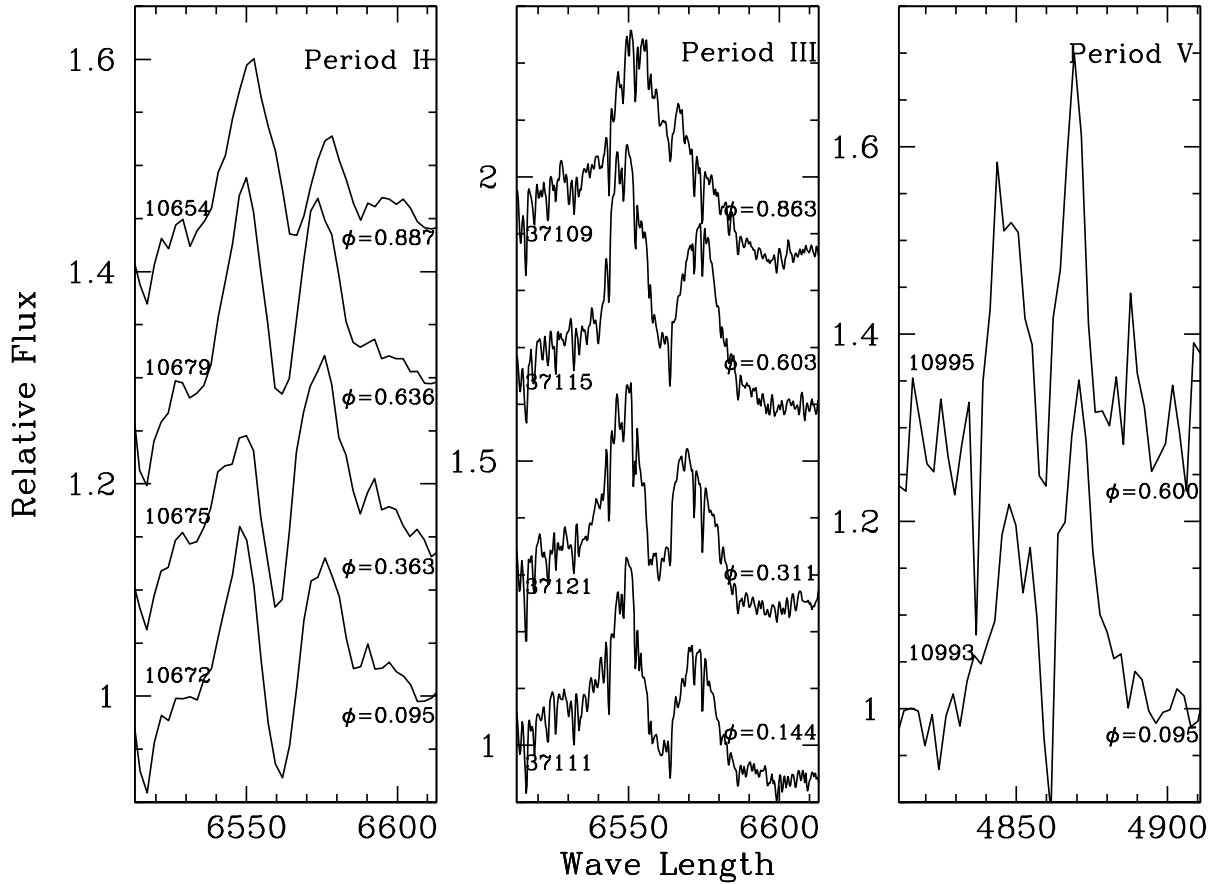


Fig. 11. Typical profile variations of $H\alpha$ in period II (left panel) and period III (mid panel) and $H\beta$ in period V (left panel) in an orbital period. The stronger peak varies between the red peak and the blue peak in period II (early-superhump era), but one of the peaks dominates through the orbital phase during periods III and V (genuine-superhump era).

tected in the spectrum in the period V, nor in the period VI, indicating the low temperature around the boundary layer insufficient to strongly irradiate the outer disk. The Na I absorption also can not be seen, while this line stayed persistent during the main outburst. These two differences of the spectral feature between in the main outburst and in the rebrightening phase may have the same origin, although the excitation potential of these species is quite different.

7. Summary and Conclusions

Here we briefly summarize what we spectroscopically observed in optical from the rising phase to the rebrightening phase of the 2001 outburst of WZ Sge, and what was revealed by detailed analyses of the data and comparison of this outburst and the previous outbursts.

- The variations of the outburst shape and the quiescence duration suggest an increasing trend of the mass transfer rate in these several tens of years. The secondary star may still have magnetic activities, though the secondary has been supposed to be

(close to) a degenerate star. (section 6.1)

- The radial velocities of the H and He emission/absorption lines measured in the main outburst had semi-amplitudes larger than those in quiescence, and the red-to-violet crossing times of these lines corresponded to $\phi \sim 0.11$. These may be interpreted to suffer from an effect of the spiral-arm structures in the accretion disk. (section 6.2)
- Na I D was found to be in strong absorption from the 1st day to, at least, 15th day of the outburst. The semi-amplitude of the radial velocity variation of this line is limited to be within 25 km s^{-1} , which is smaller than that of the white dwarf. A cool region might exist around the center of mass of this system, or the origin of this line may be the circumstellar part of the disk. This absorption line was seen not only in WZ Sge stars (WZ Sge and EG Cnc), but also in an eclipsing SU UMa star, IY UMa in superoutburst. (section 4, 5.1, 5.3, 6.2)
- Emergence of the high-excitation emission lines of He, C, and N, and the evolution from absorption to emission of $H\alpha$ between ~ 12 hours and ~ 6 hours be-

fore the outburst maximum is a new evidence of the outside-in type outburst due to the disk instability. The strong emission lines of C IV/N IV around 5800 Å were first detected in the spectrum of dwarf novae, but disappeared by the 5th day of the outburst. The emission lines of He II 4686, C III/N III, and H α is supposed to originate from the chromosphere of the accretion disk formed by irradiation. (section 4.1, 5.1, 6.3)

- The peak separations of H α and He II 4686 were about 700 km s⁻¹, which is a half of that of H α in quiescence, at the very early phase of the outburst. This implies that the accretion disk extended to have a circumstellar part. However, the phase coverage of our data are not sufficient for deriving the representative peak separation, and it is not clear whether the peak separation is naively used for measurement of the disk radius, especially around the outburst maximum (section 4.1, 5.1, 6.4)
- During the period of genuine superhumps (the latter half of the main outburst and the rebrightening phase), one of the double peaks of the Balmer emission lines dominated throughout one orbital phase, and the stronger peak interchanged in a time scale of days. These represent the eccentricity of the accretion disk, which agrees with the tidal instability model of the superhump. Such characteristics were not found in the first half of the main outburst, at least four days before the emergence of the genuine superhump (8 days after the outburst maximum), when early superhumps were dominant periodic signals. The eccentricity of the disk abruptly grew during this 4-day interval. (section 6.5)
- During the rebrightening phase, the spectra showed absorption lines of H and He I at the maximum and emission lines of the same species at the bottom, which means that the state transition of the disk was due to propagation of the heating/cooling waves, as in normal outbursts of usual dwarf novae. There was no hints of the high-excitation lines and the Na I absorption during this phase. (section 4.5, 4.6, 5.1, 6.6)
- Comparison of our spectra and those in the previous outbursts of WZ Sge indicates that the spectral feature and its evolution are different in each outburst. We need further observations in future outbursts to reveal the whole nature of the king of dwarf novae. (section 4, 5.2)

Finally, we would like to call the readers' attention for the emission lines of He II. In some spectra, e.g. figures 2 and 3, He II are seen as emission lines, whereas He I and H I are absorptions. If we use the intensity ratio of the emission lines of He II 4686/H β of these spectra to estimate the helium abundance, we will have an abundance of infinity, because there is no emission of H β .

Recently, Iijima (2002) estimated the helium abundance of a recurrent nova U Sco using the intensity ratios of He I/H I, and obtained as N(He)/N(H) = 0.16 by number, which is normal among cataclysmic variables. On

the other hand, extremely high helium abundances of the same object have been derived using the intensity ratios of He II/H I, e.g. 0.4 (Anupama, Dewangan 2000), 2.0 (Barlow et al. 1981), and 4.5 (Evans et al. 2001). The mystery of the helium abundance of U Sco might be due to a similar effect. It seems to be rather risky to estimate the helium abundances of cataclysmic variables using only the intensity ratios of He II/H I.

The authors are thankful to amateur observers for reporting the detection of this outburst their and continuous observations to VSNET. Those reports enabled us to observe the most enigmatic dwarf nova WZ Sge in a very precious phase before the maximum of a quite infrequent outburst and to easily relate the spectral feature with the state of the accretion disk. Sincere thanks are also to Warren Skidmore and Yoji Osaki for their valuable comments and discussions.

References

- Ak, T., Ozkan, M. T., & Mattei, J. A. 2001, *A&A*, 369, 882
 Anupama, G. C. & Dewangan, G. C. 2000, *AJ*, 119, 1359
 Augusteijn, T. 1994, *A&A*, 292, 481
 Baba, H., Sadakane, K., Norimoto, Y., & Ayani, K. 2001, *IAU Circ.*, 7672
 Baba, H., Sadakane, K., Norimoto, Y., Ayani, K., Ioroi, M., Matsumoto, K., Nogami, D., Makita, M., & Kato, T. 2002, *PASJ*, 54, L7
 Bailey, J. 1979, *MNRAS*, 189, 41P
 Barker, J. & Kolb, U. 2003, *MNRAS*, 340, 623
 Barlow, M. J., Brodie, J. P., Brunt, C. C., Hanes, D. A., Hill, P. W., Mayo, S. K., Pringle, J. E., Ward, M. J., et al. 1981, *MNRAS*, 195, 61
 Barwig, H., Mantel, K. H., & Ritter, H. 1992, *A&A*, 266, L5
 Bianchini, A. 1990, *AJ*, 99, 1941
 Bohusz, E. & Udalski, A. 1979, *Inf. Bull. Variable Stars*, 1583
 Brosch, N. 1979, *Inf. Bull. Variable Stars*, 1693
 Brosch, N., Leibowitz, E. M., & Mazeh, T. 1980, *ApJL*, 236, L29
 Buat-Ménard, V. & Hameury, J.-M. 2002, *A&A*, 386, 891
 Buat-Ménard, V., Hameury, J.-M., & Lasota, J.-P. 2001, *A&A*, 366, 612
 Cannizzo, J. K. 2001, *ApJL*, 561, L175
 Ciardi, D. R., Howell, S. B., Hauschildt, P. H., & Allard, F. 1998, *ApJ*, 504, 450
 Crampton, D., Hutchings, J. B., & Cowley, A. P. 1979, *ApJ*, 234, 182
 Downes, R. A. & Margon, B. 1981, *MNRAS*, 197, 35P
 Eskioglu, A. N. 1963, *Ann. d'Astrophys.*, 26, 331
 Evans, A., Krautter, J., Vanzi, L., & Starrfield, S. 2001, *A&A*, 378, 132
 Fabian, A. C., Pringle, J. E., Whelan, J. A. J., & Stickland, D. J. 1980, *MNRAS*, 191, 457
 Faulkner, J. 1971, *ApJL*, 170, L99
 Fried, R. E., Kemp, J., Patterson, J., Skillman, D. R., Retter, A., Leibowitz, E., & Pavlenko, E. 1999, *PASP*, 111, 1275
 Friedjung, M. 1981, *A&A*, 99, 226
 Gilliland, R. L. & Kemper, E. 1980, *ApJ*, 236, 854
 Gilliland, R. L., Kemper, E., & Suntzeff, N. 1986, *ApJ*, 301, 252

- Hameury, J.-M., Dubus, G., Lasota, J.-P., & Menou, K. 1999, in *Disk Instabilities in Close Binary Systems*, ed. S. Mineshige, & J. C. Wheeler (Tokyo: Universal Academy Press), 237
- Hameury, J.-M., Lasota, J.-P., & Huré, J. M. 1997, *MNRAS*, 287, 937
- Hameury, J.-M., Lasota, J.-P., & Warner, B. 2000, *A&A*, 353, 244
- Heiser, A. M. & Henry, G. W. 1979, *Inf. Bull. Variable Stars*, 1559
- Hellier, C. 2001, *PASP*, 113, 469
- Hessman, F. V., Mantel, K.-H., Barwig, H., & Schoembs, R. 1992, *A&A*, 263, 147
- Hempel, K. 1946, *IAU Circ.*, 1054
- Honey, W. B., Charles, P. A., Whitehurst, R., Barrett, P. E., & Smale, A. P. 1988, *MNRAS*, 231, 1
- Howell, S. B., Adamson, A., & Steeghs, D. 2003, *A&A*, 399, 219
- Howell, S. B., DeYoung, J. A., Mattei, J. A., Foster, G., Szkody, P., Cannizzo, J. K., Walker, G., & Fierce, E. 1996, *AJ*, 111, 2367
- Ichikawa, S., Hirose, M., & Osaki, Y. 1993, *PASJ*, 45, 243
- Iijima, T. 2002, *A&A*, 387, 1013
- Ishioka, R., Kato, T., Uemura, M., Iwamatsu, H., Matsumoto, K., Stubbings, R., Mennickent, R., Billings, G. W., et al. 2001a, *PASJ*, 53, 905
- Ishioka, R., Uemura, M., Matsumoto, K., Kato, T., Ayani, K., Yamaoka, H., Ohshima, T., Maehara, H., & Watanabe, T. 2001b, *IAU Circ.*, 7669
- Ishioka, R., Uemura, M., Matsumoto, K., Ohashi, H., Kato, T., Masi, G., Novak, R., Pietz, J., et al. 2002, *A&A*, 381, L41
- Ishioka, R., Uemura, M., Ohashi, H., Kato, T., Nogami, D., Baba, H., Makita, M., Pietz, J., et al. 2004, in preparation
- Kato, T. 2001, *Inf. Bull. Variable Stars*, 5110
- Kato, T. 2002a, *PASJ*, 54, L11
- Kato, T. 2002b, *A&A*, 384, 206
- Kato, T., Ishioka, R., & Uemura, M. 2002, *PASJ*, 54, 1029
- Kato, T., Ishioka, R., Uemura, M., Matsumoto, K., Ohashi, H., Masi, G., Good, G. A., Pietz, J., & Moilanen, M. 2001a, *IAU Circ.*, 7672
- Kato, T., Nogami, D., Baba, H., Matsumoto, K., Arimoto, J., Tanabe, K., & Ishikawa, K. 1996, *PASJ*, 48, L21
- Kato, T., Ohashi, H., Ishioka, R., Uemura, M., Matsumoto, K., Masi, G., Starkey, D., Pietz, J., & Martin, B. 2001b, *IAU Circ.*, 7678
- Kato, T., Sekine, Y., & Hirata, R. 2001c, *PASJ*, 53, 1191
- Kato, T. & Starkey, D. R. 2002, *Inf. Bull. Variable Stars*, 5358
- Kato, T., Uemura, M., Ishioka, R., Nogami, D., Kunjaya, C., Baba, H., & Yamaoka, H. 2003, *PASJ*, in press (*astro-ph/0310209*)
- King, A. R. 1988, *QJRAS*, 29, 1
- Knigge, C., Hynes, R. I., Steeghs, D., Long, K. S., Araujo-Betancor, S., & Marsh, T. R. 2002, *ApJL*, 580, L151
- Kraft, R. P. 1961, *Science*, 134, 1433
- Kraft, R. P., Mathews, J., & Greenstein, J. L. 1962, *ApJ*, 136, 312
- Krzeminski, W. 1962, *PASP*, 74, 66
- Krzeminski, W. & Kraft, R. P. 1964, *ApJ*, 140, 921
- Kuulkers, E., Knigge, C., Steeghs, D., Wheatley, P. J., & Long, K. S. 2002, in *The Physics of Cataclysmic Variables and Related Objects*, ed. B. T. Gänsicke, K. Beuermann, & K. Reinsch (San Francisco: ASP), 443
- Landolt, A. U. 2001, *IAU Circ.*, 7670
- Lasota, J.-P. 2001, *New Astron. Rev.*, 45, 449
- Lasota, J.-P., Kuulkers, E., & Charles, P. 1999, *MNRAS*, 305, 473
- Leibowitz, E. M. 1993, *ApJL*, 411, L29
- Leibowitz, E. M. & Mazeh, T. 1981, *ApJ*, 251, 214
- Lin, D. N. C. & Papaloizou, J. 1979, *MNRAS*, 186, 799
- Littlefair, S. P., Dhillon, V. S., Howell, S. B., & Ciardi, D. R. 2000, *MNRAS*, 313, 117
- Littlefair, S. P., Dhillon, V. S., & Martin, E. L. 2003, *MNRAS*, 340, 264
- Liu, W., Li, Z. Y., & Hu, J. Y. 1998, *Ap&SS*, 257, 183
- Long, K. S., Froning, C. S., Gänsicke, B., Knigge, C., Sion, E. M., & Szkody, P. 2003, *ApJ*, 591, 1172
- McLaughlin, D. B. 1953, *ApJ*, 117, 279
- Marsh, T. R. & Horne, K. 1988, *MNRAS*, 235, 269
- Mason, E., Skidmore, W., Howell, S. B., Ciardi, D. R., Littlefair, S., & Dhillon, V. S. 2000, *MNRAS*, 318, 440
- Matsumoto, K., Nogami, D., Kato, T., & Baba, H. 1998, *PASJ*, 50, 405
- Mattei, J. A., Poyner, G., Reszelski, M., McGee, H., Jones, C., Schmeer, P., Bouma, R. J., Vohla, F., et al. 2001, *IAU Circ.*, 7669
- Mayall, M. W. 1946, *Bull. Harv. Coll. Obs.*, 918, 3
- Mennickent, R. E. & Diaz, M. P. 2002, *MNRAS*, 336, 767
- Mennickent, R. E., Tappert, C., Gallardo, R., Duerbeck, H. W., & Augusteijn, T. 2002, *A&A*, 395, 557
- Meyer, F. & Meyer-Hofmeister, E. 1999, *A&A*, 341, L23
- Meyer-Hofmeister, E., Meyer, F., & Liu, B. F. 1998, *A&A*, 339, 507
- Mineshige, S., Liu, B., Meyer, F., & Meyer-Hofmeister, E. 1998, *PASJ*, 50, L5
- Misselt, K. A. 1996, *PASP*, 108, 146
- Montgomery, M. M. 2001, *MNRAS*, 325, 761
- Nather, R. E. 1978, *PASP*, 90, 477
- Nogami, D., Baba, H., Matsumoto, K., & Kato, T. 2003a, *PASJ*, 55, 483
- Nogami, D., Kato, T., Baba, H., Matsumoto, K., Arimoto, J., Tanabe, K., & Ishikawa, K. 1997a, *ApJ*, 490, 840
- Nogami, D., Masuda, S., & Kato, T. 1997b, *PASP*, 109, 1114
- Nogami, D., Uemura, M., Ishioka, R., Kato, T., Torii, K., Starkey, D. R., Tanabe, K., Vanmunster, T., et al. 2003b, *A&A*, 404, 1067
- Ogilvie, G. I. 2002, *MNRAS*, 330, 937
- Ortolani, S., Rafanelli, P., Rosino, L., & Vittone, A. 1980, *A&A*, 87, 31
- Osaki, Y. 1995, *PASJ*, 47, 47
- Osaki, Y. 2003, *PASJ*, 55, 841
- Osaki, Y. & Meyer, F. 2002, *A&A*, 383, 574
- Osaki, Y. & Meyer, F. 2003, *A&A*, 401, 325
- Osaki, Y., Meyer, F., & Meyer-Hofmeister, E. 2001, *A&A*, 370, 488
- Paczynski, B. 1967, *Acta Astron.*, 17, 287
- Papaloizou, J. & Pringle, J. E. 1979, *MNRAS*, 189, 293
- Patterson, J. 1979, *AJ*, 84, 804
- Patterson, J. 1980, *ApJ*, 241, 235
- Patterson, J. 2001, *PASP*, 113, 736
- Patterson, J., Augusteijn, T., Harvey, D. A., Skillman, D. R., Abbott, T. M. C., & Thorstensen, J. 1996, *PASP*, 108, 748
- Patterson, J., Kemp, J., Skillman, D. R., Harvey, D. A., Shafter, A. W., Vanmunster, T., Jensen, L., Fried, R., et al. 1998a, *PASP*, 110, 1290
- Patterson, J., McGraw, J. T., Coleman, L., & Africano, J. L. 1981, *ApJ*, 248, 1067

- Patterson, J., McGraw, J. T., Nather, R., & Stover, R. 1978, IAU Circ., 3311
- Patterson, J., Masi, G., Richmond, M. W., Martin, B., Beshore, E., Skillman, D. R., Kemp, J., Vanmunster, T., et al. 2002, PASP, 114, 721
- Patterson, J., Richman, H., Kemp, J., & Mukai, K. 1998b, PASP, 110, 403
- Provencal, J. L. & Nather, R. E. 1997, in Proceedings of the 10th European Workshop on White Dwarfs, ed. J. Isern, M. Hernanz, & E. Garcia-Berro (Dordrecht: Kluwer Academic Publishers), 67
- Pych, W. & Olech, A. 1995, Acta Astron., 45, 385
- Robinson, E. L., Nather, R. E., & Patterson, J. 1978, ApJ, 219, 168
- Rosenzweig, P., Mattei, J., Kafka, S., Turner, G. W., & Honeycutt, R. K. 2000, PASP, 112, 632
- Sion, E. M., Gänsicke, B. T., Long, K. S., Szkody, P., Cheng, F., Howell, S. B., Godon, P., Welsh, W. F., et al. 2003, ApJ, 592, 1137
- Skidmore, W., Clark, D., Wood, J. H., & Welsh, W. F. 2004, MNRAS, in preparation
- Skidmore, W., Mason, E., Howell, S. B., Ciardi, D. R., Littlefair, S., & Dhillon, V. S. 2000, MNRAS, 318, 429
- Skidmore, W., Welsh, W. F., Wood, J. H., Catalán, M. S., & Horne, K. 1999, MNRAS, 310, 750
- Skidmore, W., Welsh, W. F., Wood, J. H., & Stiening, R. F. 1997, MNRAS, 288, 189
- Skidmore, W., Wynn, G. A., Leach, R., & Jameson, R. F. 2002, MNRAS, 336, 1223
- Smak, J. 1993, Acta Astron., 43, 101
- Smak, J. 2002, Acta Astron., 52, 263
- Steavenson, W. H. 1950, MNRAS, 110, 623
- Steeghs, D., Marsh, T., Knigge, C., Maxted, P. F. L., Kuulkers, E., & Skidmore, W. 2001a, ApJL, 562, L145
- Steeghs, D., Marsh, T., Kuulkers, E., & Skidmore, W. 2001b, IAU Circ., 7675
- Szkody, P., Silber, A., Sion, E., Downes, R. A., Howell, S. B., Costa, E., & Moreno, H. 1996, AJ, 111, 2379
- Targan, D. 1979, Inf. Bull. Variable Stars, 1539
- Thorstensen, J. R., Patterson, J. O., Kemp, J., & Vennes, S. 2002, PASP, 114, 1108
- Vila, S. C. 1971a, Nature, 230, 39
- Vila, S. C. 1971b, ApJ, 168, 217
- Vogt, N. 1982, ApJ, 252, 653
- Wagner, R. M., Thorstensen, J. R., Honeycutt, R. K., Howell, S. B., Kaitchuck, R. H., Kreidl, T. J., Robertson, J. W., Sion, E. M., & Starrfield, S. G. 1998, AJ, 115, 787
- Walker, M. F. & Bell, M. 1980, ApJ, 237, 89
- Warner, B. 1988, Nature, 336, 129
- Warner, B., Livio, M., & Tout, C. A. 1996, MNRAS, 282, 735
- Warner, B. & Nather, E. R. 1972, MNRAS, 156, 297
- Welsh, W. F., Skidmore, W., Wood, J. H., Cheng, F. H., & Sion, E. M. 1997, MNRAS, 291, 57P
- Wheatley, P. J., Kuulkers, E., Drake, J. J., Kaastra, J. S., Mauche, C. W., Starrfield, S. G., & Wagner, R. M. 2001, IAU Circ., 7677
- Wu, X., Li, Z., Gao, W., & Leung, K. 2001, ApJL, 549, L81